



# The Late Miocene Talpidae (Eulipotyphla, Mammalia) from the Pannonian Region, Slovakia

Florentin Cailleux,<sup>1,2\*</sup>  Lars W. van den Hoek Ostende,<sup>2</sup> and Peter Joniak<sup>1</sup> 

<sup>1</sup>Comenius University in Bratislava, Faculty of Natural Sciences, Department of Geology and Paleontology, Ilkovičova 6, Mlynská dolina G, SK–842 15 Bratislava, Slovakia. <[florentin.cailleux@naturalis.nl](mailto:florentin.cailleux@naturalis.nl)>, <[peter.joniak@uniba.sk](mailto:peter.joniak@uniba.sk)>

<sup>2</sup>Naturalis Biodiversity Center, Darwinweg 2, 2333 CR Leiden, The Netherlands. <[lars.vandenhoekestende@naturalis.nl](mailto:lars.vandenhoekestende@naturalis.nl)>

**Non-technical Summary.**—The family Talpidae (moles) is a family of insectivores displaying a wide range of locomotor habits and consisting of semi-aquatic, terrestrial, and fossorial species. Although the modern diversity of Talpidae is relatively low, the paleodiversity of Talpidae during the Late Miocene (from about 11.5 to about 5.5 million years ago) was extremely high, especially in Central Europe. This is confirmed by the identification of eleven talpid species in several localities from Slovakia, including a new species of desman, *Archaeodesmana dissona* new species. Whereas the terrestrial moles are commonly found in all localities, the fossorial talpids are almost restricted to the earliest part of the Late Miocene, the Vallesian (from about 11.5 to about 9.0 million years ago). On the other hand, the desmans progressively became dominant in the beginning of the Turolian (from about 9.0 to about 5.5 million years). The high diversity of Talpidae in Central Europe is explained by the high resources and heterogeneous environments of the region, somehow reducing the pressure of competition for morphologically and ecologically similar species. The evolution of the talpid fauna reflects the environmental changes that occurred in Slovakia between the Vallesian and the Turolian. Additionally, new information has been obtained on the morphology and phylogeny of the identified species, which are: *Desmanella rietscheli*, *Desmanella dubia*, *Archaeodesmana vinea*, *Archaeodesmana dissona* n. sp., *Gerhardstorchia biradicata*, *Gerhardstorchia* sp., *Proscapanus minor*, *Proscapanus austriacus*, *Talpa* cf. *T. minuta*, Urotrichini gen. and sp. indet., and *Desmanodon* cf. *D. fluegeli*.

**Abstract.**—Central Europe is an area of high diversity for the Talpidae (Eulipotyphla, Mammalia) during the Late Miocene. The assemblages from Slovakia (Borský Svätý Jur, Krásno, Pezinok, Šalgovce, Studienka, Triblavina) are no exception with their abundant material representing eleven species. The urospiline *Desmanella* is represented by *D. rietscheli* and *D. dubia*. Desmanini fossils are attributed to *Archaeodesmana vinea*, *Archaeodesmana dissona* new species, *Gerhardstorchia biradicata*, and *Gerhardstorchia* sp. The scalopines *Proscapanus minor* and *P. austriacus* are well recorded in the Vallesian localities and support the emergence of *P. austriacus* before the MN9/10 transition. Talpini and Urotrichini are especially rare and only represented by *Talpa* cf. *T. minuta* and Urotrichini gen. sp. indet. Finally, we identified the youngest occurrence of *Desmanodon* in Europe, *D.* cf. *D. fluegeli*, at the MN9 locality of Borský Svätý Jur. The high diversity in the Late Miocene Central European is partly explained by the co-occurrence of the competing Scalopini and Talpini during the Vallesian, indicating high resource environments. The decline of these tribes, followed by the success of the desmans during the Turolian, appears as a consequence of regional environmental changes.

UUID: <http://zoobank.org/a3eb532b-c341-489a-b0ff-ecf3f9466a76>

## Introduction

Talpidae displays a wide range of locomotor habits, from terrestrial ambulatory to swimming and various degrees of fossoriality. Observation of the fossorial and semiaquatic *Condylura* even revealed climbing abilities (e.g., Norris and Kilpatrick, 2007). The locomotor habits of Talpidae have a strong phylogenetic association, some being characteristics of subgroups and others subject to strong convergence (e.g., Piras et al., 2012; Schwermann and Thompson, 2015; Sansalone et al.,

2018). The diversity of postcranial morphotypes allowed the Talpidae to fill and explore new ecological niches, which surely led to an increase of competition for specialization and, consequently, an increase of local diversity.

In heterogeneous and resource-rich areas, the diversity of Talpidae is therefore expected to be high. This assumption can barely be tested in modern faunas because Talpidae now display a low diversity. In contrast, the Miocene and Early Pliocene diversity of Talpidae at a single site was usually high in Europe, exceptionally reaching 10 species in the Late Miocene of Schemham, Austria (Ziegler, 2006a, b), and up to eleven species in the Early Pliocene of Wolfersheim, Germany (Dahlmann, 2001). Neither of these two examples is a fissure filling, where

\*Corresponding author.

the specific paleodiversity of Talpidae is overall higher (Ziegler, 2003), but probably related to taphonomic biases. The paleodiversity of Talpidae appears to be a good indicator of local resources and ecological richness.

The Late Miocene localities of Slovakia have yielded abundant material of Eulipotyphla, of which the Erinaceidae and Dimylidae recently have been described (Cailleux et al., 2023). As a second step, the present paper aims to investigate the diversity of Talpidae from the Slovak part of the Vienna and Danube basins, and their relationship to the talpid assemblages of adjacent regions.

## Material and methods

The studied material derives from six Late Miocene localities: Borský Svätý Jur (MN9), Studienka A and E (MN9), Pezinok (MN10), Triblavina (MN11), Krásno (MN11), and Šalgovce 4 and 5 (MN12) (ages according to Joniak, 2005, 2016; Šujan et al., 2016; Joniak and Šujan, 2020; Sabol et al., 2021; Cailleux et al., 2023). The geological setting has been summarized by Cailleux et al. (2023).

The material described here encompasses 396 dentognathic specimens and two humeri. The terminology and measurements methods are presented in Figure 1. Within Talpidae, the identification process of Desmanini mostly relies on the measurement method of Rümke (1985), which is followed here. According to the dental terminology of Rümke, the most posterolingual cusp on upper molars is called ‘metaconule’, which has been used in numerous taxonomic works dealing with desmans (e.g., Dahlmann, 2001; Ziegler, 2005, 2006a; Furió, 2007; Minwer-Barakat et al., 2020); this structure is referred to as the ‘hypocone’ in all other talpid groups. We prefer to unify the dental terminology of all talpid groups, and thus systematically use the term ‘hypocone’ (Fig. 1). To avoid any confusion, the term ‘metaconule’ is used in parentheses when referring to desmans. We mainly follow van den Hoek Ostende (1989) and Klietmann (2013) for the dental terminology of other Talpidae. In all cases, we prefer the use of lophid instead of cristid for paralophid and protolophid (Fig. 1).

We use the measurement protocol of Furió (2007) for *Desmanella*, because this method appeared accurate (García-Alix et al., 2011). We follow Hutchison (1974) for other talpids. We note that the Austrian material described by Ziegler (2006a) was measured with a modified version of the Hutchison method for upper molars, which led to slightly larger values for length and width. We took new measurements for the type material of *Proscapanus minor* Ziegler, 2006a, and *Proscapanus austriacus* Ziegler, 2006a, for comparison purposes. The measurement method and terminology for postcranial elements follow Klietmann (2013).

All measurements are given in millimeters (mm). The dental elements were measured using a digital measuring microscope with a mechanical stage and digital measuring clocks. The identification numbers, laterality, and measurements of specimens are provided in Supplementary Data 1. Specimens in figures are represented in left orientation. Reversed specimens are indicated by an underlined number. Unless otherwise noted, SEM pictures are made in occlusal view. Drawings were

obtained with a graphic tablet (Wacom Intuos Pro) and the software Autodesk SketchBook (v. 8.7.1). All the described specimens are housed at the Department of Geology and Paleontology of Comenius University, Bratislava.

*List of abbreviations.*—H = height; L = length; Ltt = length to tuberculum teres posterior; Lpt = length to pectoral tubercle; Ltm = length to Tuber major; Wcf = width from capitulum to fossa; Mdd = minimum diaphysis diameter; Mdd ref = minimum diaphysis diameter parallel to reference line; N = number of specimens; W = width; W1 = anterior width; W2 = posterior width.

*List of localities.*—BJ, Borský Svätý Jur; KR, Krásno; PK, Pezinok; SG, Šalgovce; ST, Studienka; TB, Triblavina.

*Repositories and institutional abbreviations.*—AMPG = Athens Museum of Palaeontology and Geology, Greece; LMJG = Landesmuseum Joanneum of Graz, Austria; NHMV = Natural History Museum of Vienna, Austria; SMF = Senckenberg Research Institute and Natural History, Frankfurt, Germany.

## Systematic paleontology

Order Eulipotyphla Waddell, Okada, and Hasegawa, 1999  
Family Talpidae Fischer, 1814  
Subfamily Uropsilinae Dobson, 1883  
Genus *Desmanella* Engesser, 1972

*Type species.*—*Desmanella stehlini* Engesser, 1972.

*Other species.*—*Desmanella crusafonti* Rümke, 1974; *D. fejfari* Gibert, 1975; *D. dubia* Rümke, 1976; *D. amasyae* Engesser, 1980; *D. cingulata* Engesser, 1980; *D. sickenbergi* Engesser, 1980; *D. engesseri* Ziegler, 1985; *D. gardiolensis* Crochet, 1986; *D. storchi* Qiu, 1996; *D. rietscheli* Storch and Dahlmann, 2000; *D. woelfersheimensis* Dahlmann, 2001; and *D. gudrunae* van den Hoek Ostende and Fejfar, 2006.

*Diagnosis.*—See Engesser (1972, p. 80).

*Occurrence.*—Late Oligocene to Late Pliocene of Europe (Engesser, 1972; Crochet, 1986; Ziegler, 1998; Dahlmann, 2001). Also identified in the Miocene of Asia (Engesser, 1980; Qiu, 1996).

*Desmanella rietscheli* Storch and Dahlmann, 2000, and *Desmanella* cf. *D. rietscheli* Storch and Dahlmann, 2000  
Figure 2.1–2.20; Table 1

*Holotype.*—Left M1, SMF 75/485, Dorn-Dürkheim, Germany (Storch and Dahlmann, 2000).

*Diagnosis.*—See Storch and Dahlmann (2000, p. 65).

*Occurrence.*—From MN9 to MN11 of Central Europe (Storch and Dahlmann, 2000; Fejfar and Sabol, 2005; Ziegler, 2006a) and MN10 of France (Ménouret and Mein, 2008).

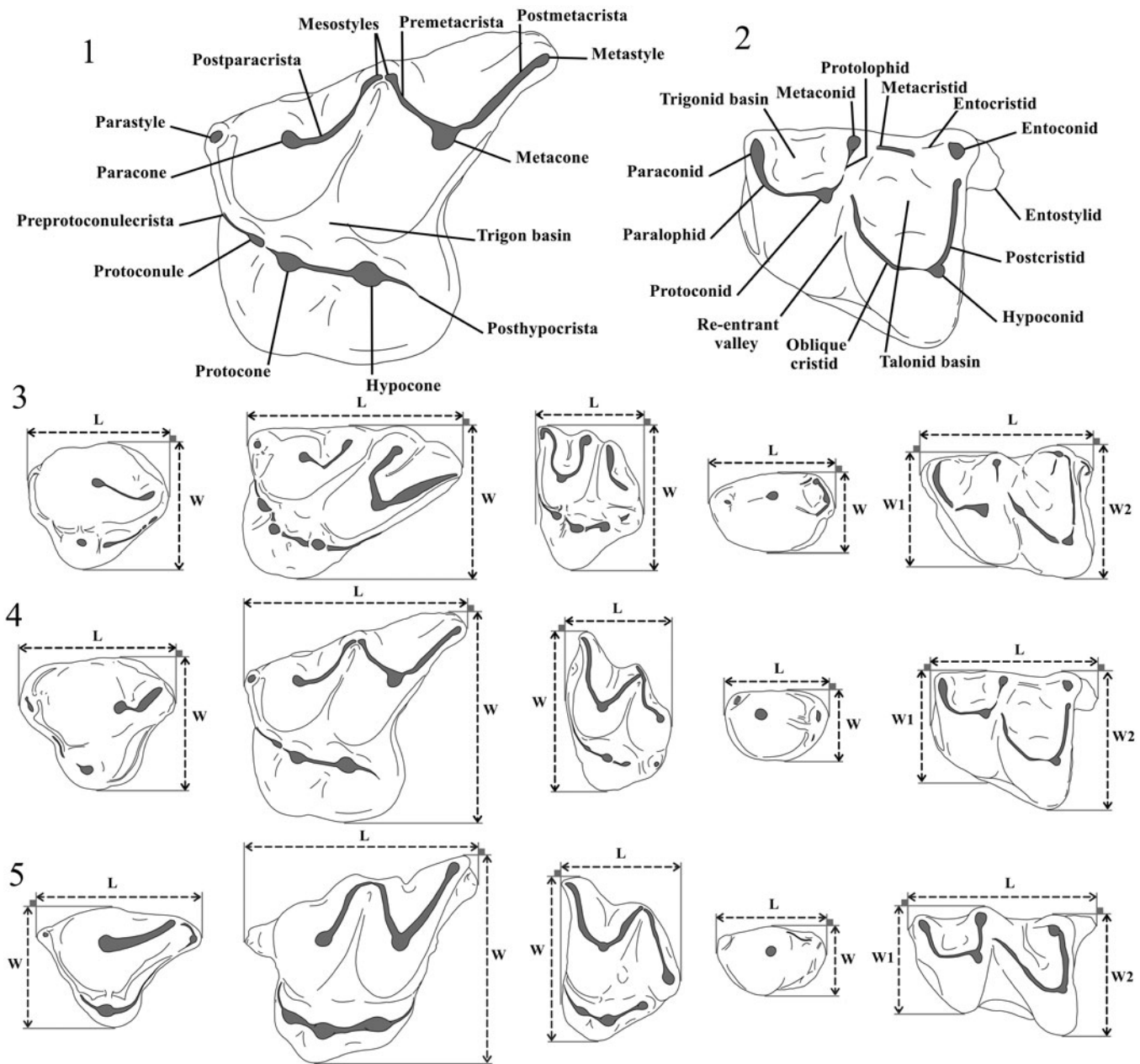


**Figure 1.** Terminology used for the (1) M1 and (2) m1 of Talpidae, and measurements protocol for P4, M1, M3, p4, and m1 of (3) Desmanini, (4) *Desmanella*, and (5) other Talpidae. L = Length; W = width; W1 = anterior width; W2 = posterior width.

**Description.**—The I1 shows an asymmetry with a convex anterodistal face and concave posteromesial face (Fig. 2.1). From the central main cusp extends an anteromesial crest reaching the anterior margin. A shorter and lower posterior crest connects the base of the cusp to the posterior margin. Narrow posteromesial and posterodistal cingula are present.

The P3 is a two-rooted ovoid premolar with a main cusp in anterior position. A sharp and high crest extends from its tip to the posterior margin of the tooth. A short cingulum is present on the posterolingual border. The P4 has a conical and central paracone. The metacone is incorporated in a short and slightly curved posterior crest. Rarely, this crest turns lingually and connects with the cingulum. A tiny parastyle is often distinguishable on the anterior cingulum (Fig. 2.6). A strong but low protocone

is found at the anterolingual margin, in a more anterior position than the paracone. A cingulum is present all around the premolar except at the most lingual and labial part. The deciduous dP4 has a short labial part and a stretched posterolingual border. The paracone is conical and situated in the middle of the labial part. The metacone is indistinct from the short postparacrista. A weak constriction separates the lingual part from the labial part on both anterior and posterior margins. A cusplule is distinguishable in the posterolingual border of the most unworn specimen (Fig. 2.5). A flat surface is present on the anterolingual side of the tooth, bordered by a broad cingulum.

The M1 is a stout three-rooted element. The high metacone is connected to a straight metastyle by a sharp postmetacrista. The premetacrista is short. The mesostyles are adjoining. The

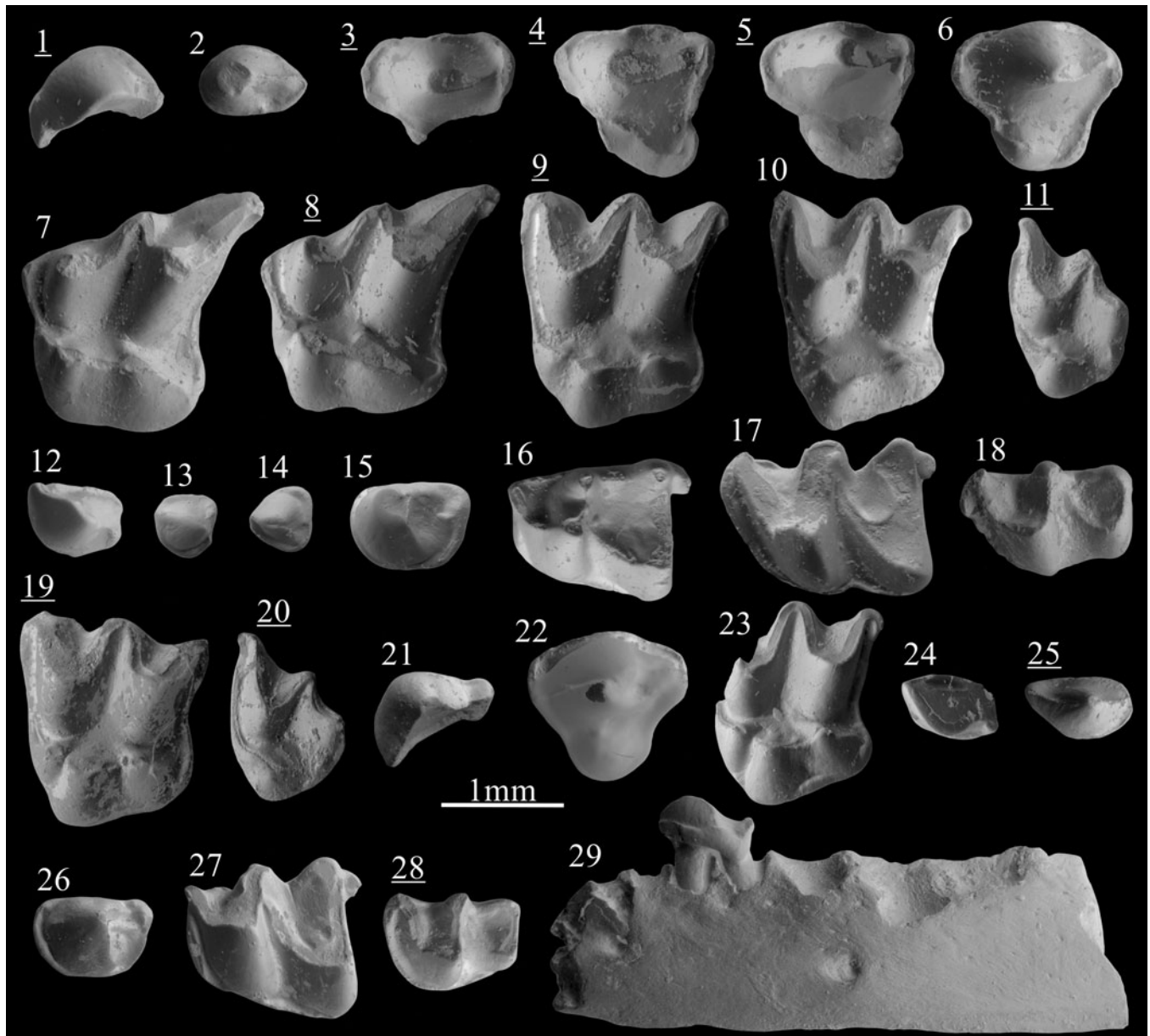


**Figure 2.** Scanning electron photomicrographs of (1–18) *Desmanella rietscheli* Storch and Dahlmann, 2000, from Borský Svätý Jur; (19, 20) *D. cf. D. dubia* Rümke, 1976, from Krásno; (21–29) *D. dubia* Rümke, 1976, from Šalgovce 5. (1) I1, BJ213250; (2) P3, BJ213340; (3) dP4, BJ213264; (4) dP4, BJ213269; (5) dP4, BJ213270; (6) P4, BJ213260; (7) M1, BJ213272; (8) M1, BJ213275; (9) M2, BJ213280; (10) M2, BJ213287; (11) M3, BJ213297; (12) I1, BJ213252; (13) p1?, BJ213253; (14) p2?, BJ213254; (15) p4, BJ213305; (16) m1, BJ213311; (17) m2, BJ213325; (18) m3, BJ213336; (19) M2, KR1270083; (20) M3, KR1270076; (21) I1, SG1980102; (22) P4, SG1980098; (23) M2, SG1980080; (24) i2, SG1980087; (25) p3, SG1980104; (26) p4, SG1980110; (27) m1, SG1980093; (28) m3, SG1980095; (29) mandible with p4, SG1980118, labial view. Images with underlined numbers are reversed.

**Table 1.** Measurements (in mm) of *Desmanella rietscheli* Storch and Dahlmann, 2000, from Borský Svätý Jur (MN9), Slovakia. L = Length; N = number of specimens; W = width; W1 = anterior width; W2 = posterior width.

	I1		P3		P4		dP4		M1		M2		M3		i2		
N	L	W	L	W	L	W	L	W	L	W	L	W	L	W	L	W	
2	2	1	1	1	5	6	3	1	4	5	4	5	4	3	2	2	
Min	0.89	0.80			1.13	1.06	1.25		1.86	1.70	1.55	1.87	0.91	1.44	0.73	0.57	
Max	1.04	0.82			1.38	1.21	1.34		2.01	1.89	1.71	1.97	0.97	1.49	0.90	0.64	
Mean	0.96	0.81	0.95	0.57	1.29	1.16	1.29	1.22	1.96	1.78	1.65	1.93	0.93	1.47	0.80	0.60	
	p1?		p2?		p3		p4		m1		m2		m3				
N	L	W	L	W	L	L	L	W	L	W1	W2	L	W1	W2	L	W1	W2
1	1	1	1	1	2	3	6	6	13	13	16	8	8	9	5	6	5
Min					0.73	0.45	0.89	0.62	1.45	0.93	1.11	1.62	1.06	1.07	1.18	0.74	0.66
Max					0.77	0.50	0.95	0.68	1.59	1.10	1.27	1.77	1.16	1.20	1.41	0.89	0.78
Mean	0.55	0.53	0.51	0.53	0.75	0.48	0.92	0.66	1.53	1.01	1.18	1.69	1.10	1.14	1.30	0.82	0.71

paracone is lower than the metacone but reaches twice the height of the mesostyles. A minute parastyle marks the angular anterolabial corner of the tooth. A thin preprotoconulecrista connects the parastyle to the base of the weak protoconule. This cusp is anterolabially attached to the protocone. The hypocone, intermediate in height between the protocone and the protoconule, is anteroposteriorly elongated. The posthypocrista ends without touching the cingulum. The hypocone lies on a strong posterior extension. The posterior basin is largely open. The outline of the posterior margin is S-shaped. The posterior cingulum is found from the metastyle to the posterior side of the hypocone (Fig. 2.7, 2.8). In three out of seven specimens from Borský Svätý Jur, this cingulum continues onto the lingual side of the hypocone. Short and narrow cingula are punctually found on the labial margin.

The M2 is a three-rooted compact tooth. The metacone is slightly higher than the paracone. The preparacrista and postmetacrista are convex, but both the parastyle and the metastyle create a small external hook. The mesostyle is undivided. The preprotoconulecrista is weak but complete. The protoconule is attached to the protocone. The latter is situated more posteriorly than the paracone. The base of the paracone is wider than in M1. The tip of the protocone is connected to the tip of the hypocone by the ridge extending over the lingual complex. The posthypocrista does not touch the cingulum. The posterolingual margin is straight. The posterior cingulum is narrow and stops at the base of the hypocone. Discontinuous cingulums can be punctually present on the most-lingual margin of the tooth.

The M3 is a small tooth, wider than long. The metacone is a transversely elongated cusp lower than the paracone. There is neither a postmetacrista nor a metastyle. Metacone and paracone are connected by adjoining mesostyles, forming a relatively pointy labial margin (Fig. 2.11). The preparacrista is short and convex before the slightly concave parastyle. The lingual part is mainly occupied by an angular protocone. A protoconule is distinguished on the less-worn specimens and is connected to the anterior cingulum. A hypocone is attached to the lingual base of the metacone. No cingulum are found other than the anterior one.

The only available fragment of mandible preserves the seven posterior alveoli. The alveoli of m2 are slightly larger than the alveoli of m1. The corpus is narrow and the foramen mandibulae is situated below the anterior root of m1. The fragment of ramus mandibulae is straight. The lowest part of the masseteric fossa consists of a low slope.

The i2 is spatulate but with an oblique orientation. A thin transverse ridge is visible, hardly reaching the posterior margin. Near this ridge a posterolabial bulge is found, from which a short and narrow distal cingulid starts. A continuous mesial cingulid connects the low posterior margin to the anterior crest.

The p1? is a small premolar with a low, sturdy cuspid. An anterior crest connects the cuspid to the anterior border before turning lingually. The posterior crest is weak but connected to a small posterior cuspule on the posterolingual margin. Broad posterolabial and anterolingual cingulids are present. The p2? can be distinguished from the p1? by its subtriangular occlusal outline, the thinner and shorter anterior crest, and the lack of posterior cuspule (Fig. 2.14 vs Fig. 2.13). The cingulid is found all along the tooth except for the anterolabial flank.

The p3 is a one-rooted asymmetrical tooth with a small conical cuspid. From its tip extends a short anterior crest turning labially at the anterior border. A low posterior crest connects the base of the cuspid to the posterior margin. Both central crests connect to the broad lingual cingulid. A posterolabial cingulid is present. The large two-rooted p4 has a robust, almost conical protoconid in an anterior position. A short talonid is present, broader on the lingual side where a longitudinal crest joins a small posterior cuspule. A complete cingulid surrounds the premolar, narrower on the most lingual and labial sides.

The m1 has a trigonid shorter than the talonid. The paraconid is included in a curved and low paralophid connected to the high protoconid. The metaconid is conical, higher than the paraconid and in a more posterior position than the protoconid. The trigonid basin consists of a slope that is open on the lingual side. The oblique cristid reaches the central part of the trigonid wall. There is no entocristid, but the entoconid is slightly elongated. The entostylid is well developed. The posterior cingulid is narrow. The labial cingulid is missing below the hypoconid and the protoconid.

The m2 differs from the m1 by usually being longer, by a wider trigonid, an oblique cristid reaching the metaconid–protoconid wall in a more lingual position, and a continuous labial and anterior cingulid (Fig. 2.17 vs Fig. 2.16). On the m3, the trigonid is wider than the talonid but has a similar length. The paraconid is not distinguishable from the low and curved paralophid. The protoconid is triangular and not compressed. The conical metaconid is isolated and situated in a slightly more posterior position than the protoconid. The talonid is reduced, with a very low hypoconid and a slightly higher entoconid. The oblique cristid is similar to that in m2. There is neither an entostylid nor a posterior cingulid. The labial and anterior cingulids are complete.

*Material.*—Borský Svätý Jur (*D. rietscheli*): two I1, one P3, nine P4, three dP4, eight M1, 17 M2, five M3, two i2, one p1?, one p2?, four p3, one fragment of mandible with p4, six p4, 16 m1, 11 m2, six m3; one fragment of edentulous mandible. Measurements are provided in Table 1.

Studienka A (*Desmanella* cf. *D. rietscheli*): one M3 (L = 0.96), one m1 (L = 1.59, W1 = 1.01, W2 = 1.07).

Studienka E (*Desmanella* cf. *D. rietscheli*): one m3 (L = 1.38, W1 = 0.99, W2 = 0.82).

*Remarks.*—Four species of *Desmanella* are identified in the late Middle Miocene to Late Miocene of Europe: *D. stehlini* from MN7/8 of Anwil (Switzerland), *D. rietscheli* from MN11 of Dorn-Dürkheim (Germany), *D. crusafonti* from MN12 of Concu (Spain), and *D. dubia* from MN12 of Pikermi (Greece). *Desmanella stehlini* is found in few MN7/8 localities (Engesser, 1972; Ziegler, 2003) and *D. dubia* in localities younger than Pikermi (Doukas et al., 1995; Vasileiadou and Doukas, 2022). However, despite the common presence of *Desmanella* during the Vallesian, material is rarely identified at the species level (e.g., Bachmayer and Wilson, 1978; Crochet and Green, 1982; Rzebik-Kowalska, 2005; Ziegler, 2006a, b; Ménouret and Mein, 2008). The taxonomic situation of the Vallesian *Desmanella* assemblages is somewhat problematic, which is a

consequence of the limited type material of *D. stehlini* and *D. rietscheli*.

The *Desmanella* from Borský Svätý Jur is not differentiable from the Austrian material identified as *Desmanella* aff. *D. rietscheli*. The use of such open nomenclature by Ziegler (2006a) was motivated by a difference in the measurements of lower molars because the Austrian specimens are narrower than the type material of the species (based on Storch and Dahlmann, 2000). This size variation is actually an artifact related to different measurement methodologies. Despite both papers mentioning the method of Hutchison (1974), Ziegler (2006a) used the occlusal surface to calculate width whereas Storch and Dahlmann (2000) apparently used the dental plane as a reference orientation, leading to a larger width. In supplementary material (S2) are provided new measurements and collection numbers of the lower molars of *D. rietscheli* from its type locality, Dorn-Dürkheim 1. These measurements show that *Desmanella* aff. *D. rietscheli* from Götzendorf, Richardhof-Wald, Schernham, and Eichkogel can be attributed to *D. rietscheli* without reservation.

Although the diagnostic features of *Desmanella rietscheli* are already found in the MN9 assemblage from Borský Svätý Jur, we noticed in our material that the protoconule on M1–M2 is relatively small and the posterior margin of M1 is sometimes less concave (e.g., Fig. 2.8). These features are exclusively found in *D. stehlini*, therefore suggesting a close affinity between *D. stehlini* and *D. rietscheli*. The material from Studienka A falls within the range of variation observed in the material described by Ziegler (2006a), but is attributed to *Desmanella* cf. *D. rietscheli* because of the limited sample size and the relatively small dimensions of the m2. Crochet and Green (1982) described *Desmanella* cf. *D. stehlini* from the MN10 of Montredon. This form is different from *D. stehlini* because of the stronger hypocones on M1 and M2 and the m1 shorter than the m2. Crochet and Green (1982) mentioned features that have later been included in the diagnosis of *D. rietscheli* by Storch and Dahlmann (2000). No differences have been found with our sample. Consequently, we reclassify this material as *Desmanella* cf. *D. rietscheli*. The material from the MN10 locality of Soblay, identified as *Desmanella* cf. *D. rietscheli* by Mérouret and Mein (2008), probably belongs to the same species.

The dentition anterior to P4/p4 can only be confidently attributed to a species when preserved in maxillary and mandible fragments (e.g., Engesser, 1980; Klietmann et al., 2015), and therefore generally is not mentioned except for a few exceptions (e.g., Dahlmann, 2001). Small premolars with low, conical cusps and developed cingulids are here attributed to p1, p2, p3, and P3 of *Desmanella rietscheli*, the former two being tentative attributions. Although the evolutionary degree of these two elements coincides with *Desmanella*, their position along the dental row cannot be fully confirmed. Nevertheless, a clear similarity is found with the deciduous teeth attributed to *D. engesseri* by Klietmann et al. (2015).

Finds of milk teeth attributed to *Desmanella* are exceedingly rare. The only described specimens so far were found in the Early Miocene of Petersbuch 28 (Klietmann et al., 2013) and attributed to *D. engesseri*. The three specimens from Borský Svätý Jur (Fig. 2.3–2.5) differ from this unique deciduous P4 by the more rounded lingual extension, but share a similar moderate

transversal elongation on which the “protocone” consists of a strengthening of the lingual cingulum.

*Desmanella dubia* Rümke, 1976  
and *Desmanella* cf. *D. dubia* Rümke, 1976  
Figure 2.21–2.29; Table 2

*Holotype*.—Right M1, AMPG PK-565, Pikermi, Greece (Rümke, 1976).

*Diagnosis*.—See Rümke (1976).

*Occurrence*.—From MN11 to MN14 of Europe (Rümke, 1976; Crochet, 1986; Harrison and Rzebik-Kowalska, 1994; Doukas et al., 1995; Furió, 2007; this paper).

*Description*.—The asymmetrical I1 is characterized by a high cusp from which extend two sharp anteromesial and posterior crests. The posterior crest reaches the base of a posterior cuspule, connected by the continuous lingual cingulum to the anterior margin. The convex distal side only bears a cingulum at its posteriormost margin.

The P4 possesses a strong, almost conical paracone. The postparacrista is laterally compressed. In one of the two specimens, the postparacrista turns lingually and connects the cingulum. The parastyle is hardly visible. The lingual extension bears a low and conical protocone. There is a complete, relatively broad cingulum.

The lingual part of M1 is broad with three well-differentiated cusps. The protoconule is as high as the protocone and both are interconnected by a thin ridge. Similarly, the protocone is connected to the hypocone by a thin crest. The protoconule and the hypocone display a short labial elevation. The posthypocrista is short and the posterior cingulum is broad.

The M2 is a robust tooth. The metacone is slightly higher than the protocone. The postmetacrista is almost straight and joins a hook-like metastyle touching the posterior cingulum (Fig. 2.23). The protoconule, from which the anterior cingulum extends, is large and slightly anterolingually compressed. A thin ridge connects it to the conical protocone. A ridge connects the protocone to the base of the large hypocone. The posthypocrista is thick and touches the cingulum in two out of three specimens. Strong anterior and posterior cingulums are present, such as a thick but short posterolingual cingulum and an anterolingual cingulum that varies in size.

The M3 is rather small. The metacone and paracone are connected by a curved crest. The preparacrista is straight. The lingual part is rounded and bears a low protocone connected to the anterior cingulum. A short and straight posterior crest extends from the protocone. The hypocone is massive and isolated. It creates a noticeable bulge on the posterior margin of the tooth.

The ramus of the mandible is straight and slightly thicker near the molars (Fig. 2.29). Three alveoli anterior to p4 are preserved, along with the p4 and four posterior alveoli corresponding to m1 and m2. The two alveoli directly anterior to the p4 have a similar ovoid shape and their total length is similar to the total length of the p4 alveoli. This indicates the presence of a single-rooted p3 and p2. The alveolus of p2 is situated

**Table 2.** Measurements (in mm) of *Desmanella* cf. *D. dubia* Rümke, 1976, from Krásno (MN11) and *Desmanella dubia* Rümke, 1976, from Šalgovce 5 (MN12), Slovakia. L = Length; N = number of specimens; W = width; W1 = anterior width; W2 = posterior width.

<i>Desmanella</i> cf. <i>D. dubia</i> , Krásno																	
	I1		P4		M2		M3		i2		p3		p4		m1		
	L	W	L	W	L	W	L	W	L	W	L	W	L	W	L	W1	W2
N	1	1	1		2	2	3	3	3	3	5	5	3	3	1	1	4
Min					1.52	1.69	0.86	1.25	0.79	0.53	0.76	0.50	0.81	0.59			1.04
Max					1.56	1.70	0.96	1.49	0.88	0.54	0.90	0.61	0.85	0.61			1.20
Mean	0.97	0.64	1.33		1.54	1.69	0.90	1.36	0.82	0.53	0.80	0.54	0.84	0.60	1.39	0.85	1.13
	m2		m3		W2		L		W1		W2						
N	1	1	1		1		1		1		1		1				
Mean	1.02	1.07	0.71		0.59												
<i>Desmanella dubia</i> , Šalgovce 5																	
	I1		P4		M2		i2		p3?		p4		m1		m2		
	L	W	L	W	L	W	L	W	L	W	L	W	L	W1	W2	W1	W2
N	3	3	2	1	1	1	2	2	6	6	6	6	1	1	4	1	3
Min	0.81	0.62	1.29				0.93	0.50	0.88	0.51	0.79	0.64			0.99		0.88
Max	0.99	0.77	1.31				0.95	0.51	0.92	0.55	1.00	0.68			1.06		0.97
Mean	0.90	0.70	1.30	1.13	1.61		0.94	0.50	0.90	0.53	0.90	0.66	1.48	0.83	1.02	0.87	0.94
	m3		L		W1		W2										
N	1	1			1		2										
Min							0.59										
Max							0.60										
Mean	1.09	0.73					0.60										

slightly more labially than the other ones. Foramina are found below the anterior alveole of the m1 and below the p2.

The tear-shaped i2 has a laterally compressed cuspid with an oblique anterior crest and a low but thick posterior ridge. The latter is split in two: the largest part of the ridge is connected to a posterior cuspule whereas the thinnest part of the ridge leads to the continuous lingual cingulid. A strong posterolabial cingulid is present.

The p3 is a one-rooted, asymmetrical tooth. Two sharp, slightly labially oriented crests connect the tip of the conical cuspid to the anterior and posterior border. A complete cingulid is present, broader on the lingual and posterior sides. The sturdy two-rooted p4 has a slightly bent protoconid in anterior position. The distinct talonid bears a central ridge. The crest at the margin of the tooth is thicker on the posterolingual side. The cingulid is continuous in two specimens but is lingually and labially interrupted in the four other complete specimens.

The m1 has a trigonid shorter than the talonid. The low paralophid is narrow. The paraconid is indistinct. The metaconid is a conical cuspid in a more posterior position than the high protoconid. The trigonid basin is widely open on the lingual side and partially bordered by a thin cingulid. The entoconid is a high, laterally compressed cuspid whereas the hypoconid is low and subtriangular in cross section. The slightly curved oblique cristid reaches the central part of the trigonid wall. There is no distinct entocristid but the talonid is closed by a low metacristid. The entostylid is strong. The posterior cingulid is narrow but always present. The labial cingulid is only slightly disrupted below the hypoconid and the protoconid.

The m2 differs from m1 by the larger trigonid, the longer protolophid, and the stronger-curved oblique cristid. The latter ends high on the trigonid wall. A connection is found between the labial and the posterior cingulid. The trigonid of m3 is wider than the talonid but has a similar length. The paraconid is indistinct from the paralophid. The metaconid is situated in a slightly more posterior position than the protoconid. The

reduced talonid has a low hypoconid, higher entoconid, and straight oblique cristid.

**Material.**—Krásno (*Desmanella* cf. *D. dubia*): one I1, four P4, one M1, four M2, eight M3, three i2, five p3, three p4, five m1, three m2, one m3. Measurements are provided in Table 2.

Šalgovce 4 (*Desmanella* cf. *D. dubia*): one I1 (L = 0.78, W = 0.60).

Šalgovce 5 (*D. dubia*): four I1, two P4, two M1, five M2, one M3, two i2, six p3, one fragment of mandible with p4, eight p4, four m1, three m2, two m3. Measurements are provided in Table 2.

**Remarks.**—Only a few features allow the distinction between *Desmanella rietscheli* and *D. dubia*. The latter has overall a more robust morphology of the M2 with a thicker hypocone, larger lingual area and less lingually elongated protocone. Both upper and lower molars have thicker and more continuous cingula. *Desmanella dubia* is also one of the smallest species of its genus. These distinctions are all found in our material. *Desmanella gardiolensis*, *D. crusafonti*, and *D. woelfersheimensis* can be differentiated from *D. dubia* by their larger to significantly larger size (Dahlmann, 2001; Furió, 2007).

Although abundant, the MN11 material from Krásno is badly preserved. The presence of *D. rietscheli* was expected because it is the only *Desmanella* species recorded during the early part of the Late Miocene (MN9–MN11) and because this species is recorded in Eichkogel and Kohfidisch (Ziegler, 2006a; this paper). However, our material has smaller dimensions than that from Eichkogel and the complete specimens are morphologically closer to the species from Šalgovce 5 than to any older and contemporaneous samples (e.g., Fig. 2.19 and Fig 2.23). Although the poor preservation in Krásno hampers a firm identification, *D. dubia* probably emerged during the MN11.

Subfamily Talpinae Fischer, 1814

Tribe Desmanini Thomas, 1912

Genus *Archaeodesmana* Topachevsky and Pashkov, 1983

*Type species.*—*Archaeodesmana pontica* (Schreuder, 1940).

*Other referred species.*—*Archaeodesmana vinea* (Storch, 1978); *A. bifida* (Engesser, 1980); *A. adroveri* (Rümke, 1985); *A. brailloni* (Rümke, 1985); *A. getica* (Terzea, 1980); *A. luteyni* (Rümke, 1985); *A. major* (Rümke, 1985); *A. turolense* (Rümke, 1985); *A. acies* Dahlmann, 2001; *A. baetica* Martín-Suárez et al., 2001; *A. primigenia* Ziegler, 2006a; *A. elvirae* Minwer-Barakat et al., 2008.

*Diagnosis.*—See Rümke (1985, p. 85), under the name *Dibolia*.

*Occurrence.*—*Archaeodesmana* is identified from MN9 of Central Europe (Ziegler, 2005, 2006a, b), in the Late Miocene and until the latest Pliocene of Europe (e.g., Rümke, 1985; Dahlmann 2001; Martín-Suárez et al., 2001).

*Remarks.*—In the paleontological literature, desmans are traditionally considered as a subfamily. However, genetic data (e.g., He et al., 2016) suggest its inclusion within the Talpinae, which is followed here. Additionally, we refer here to the genus *Archaeodesmana* Topachevsky and Pashkov, 1983, rather than *Ruemkelia* Rzebik-Kowalska and Pawłowski, 1994, an alternative name meant to replace *Dibolia* (see Rzebik-Kowalska and Rekovets, 2016). The generic attribution of *Archaeodesmana primigenia* has been considered uncertain by Ziegler (2005), based on both the lack of upper incisor and the chronological gap between this species and the other *Archaeodesmana* species. The latter problem has been resolved with the occurrence of MN9 and MN10 *Archaeodesmana* (Ziegler, 2006b; Ménouret and Mein, 2008). Despite the lack of I1, the strong similarities between *A. primigenia* and *A. vinea* leaves little doubt on the generic attribution of the former.

*Archaeodesmana vinea* (Storch, 1978)

Figure 3; Table 3

*Holotype.*—Fragment of mandible with p1, p2, p4, m1, and m2, SMF 75/1260, Dorn-Dürkheim, Germany (Storch, 1978).

*Diagnosis.*—See Rümke (1985, p. 88).

*Occurrence.*—From MN9 to MN11 of Slovakia, Austria, Germany, and France (Rümke, 1985; Mein, 1999; Ziegler, 2006b; Ménouret and Mein, 2008; this paper).

*Description.*—The I1 corresponds to the AW morphotype sensu Rümke (1985) (Fig. 3.1). This triangular tooth has an almost flat anterior face and a convex distal face. The posteromesial side is concave. The transverse crest is bilobed, the labial lobe being the stronger. The inner cingulum is hardly distinguishable. The upper canine is an elliptical two-rooted tooth with an almost straight conical cusp in its middle part. Anterior and posterior cingulums are present: the

anterior cingulum is longer, but less robust than the posterior one.

The P1 is a rounded, two-rooted tooth with a configuration similar to the upper canine. It differs by its smaller size and its less transversely compressed cusp (Fig. 3.3). A faint posterior crest is present. The anterior cingulum is short. The thick posterolingual cingulum starts in the middle of the posterior flank and almost reaches the anterior cingulum. The P2 is a big, two-rooted tooth with a strong cusp slightly inclined backwards. A thin crest is distinguishable between the tip of the cusp and the posterior border. The anterior cingulum is weak; the posterior cingulum is wide and extends lingually until the middle of the premolar. The two roots have the same dimensions. The two-rooted P3 has a more compact outline than the P2. The paracone is situated in the middle of the tooth whereas a small protocone is attached on the lingual side. The anterior, posterior, and lingual cingulums are weak. The three-rooted P4 has a central paracone with a broad base. A low crest connects it to a small, conical metacone. Smaller than the latter, the protocone is connected to the base of the paracone. Next to the protocone, a small and almost isolated accessory cusp is distinguishable. Anterior and lingual cingula are strong whereas the posterolabial cingulum is less developed.

The lingual margin of the M1 is rounded. The paracone is transversely compressed and connected to the anterior mesostyle. The postparacrista is deeply notched. The parastyle is circular and connected by a thin crest to the base of the paracone. The metacone is more transversely compressed than the paracone. The posterior mesostyle is slightly lower than the anterior mesostyle. They are separated by a deep valley. The postmetacrista is almost straight. The metastyle is lower than the two mesostyles. The protoconule is bigger than the hypocone (= metaconule) and is connected to the parastyle by a preprotoconulecrista. The robust protocone is connected by a short crest to the low accessory cusp. The protocone and the hypocone (= metaconule) are weakly separated. From the latter descends a thin posthypocrista joining the margin. The labial cingulum is discontinuous.

The only available M2 is damaged (Fig. 3.8). The paracone is more extended lingually than the metacone. The postparacrista leads to a robust anterior mesostyle. The preparacrista ends freely near an isolated and sturdy parastyle. The latter is lower than the anterior mesostyle. The protoconule is small but robust and is connected to the parastyle by a complete preprotoconulecrista. The hypocone (= metaconule) is bigger than the protoconule and is connected to the posterolabial end of the tooth. The conical protocone has a posterior crest connected to a small accessory cusp.

On M3, the paracone is connected to both the anterior mesostyle and the parastyle by a U-shaped crest. The metacone is as strong as the paracone, but more transversely compressed. The posterior mesostyle is weaker than the anterior one. The hypocone (= metaconule) is isolated and placed in a very posterior position. The protocone is strong and displays a short posterior crest in contact with the anterior base of the hypocone (= metaconule). The protoconule is strong and connected to the parastyle.

The i2 bears a high central crest in anterior position, descending posteriorly and joining a small cusplule at the posterior-most margin. The anterior flank is relatively straight. The



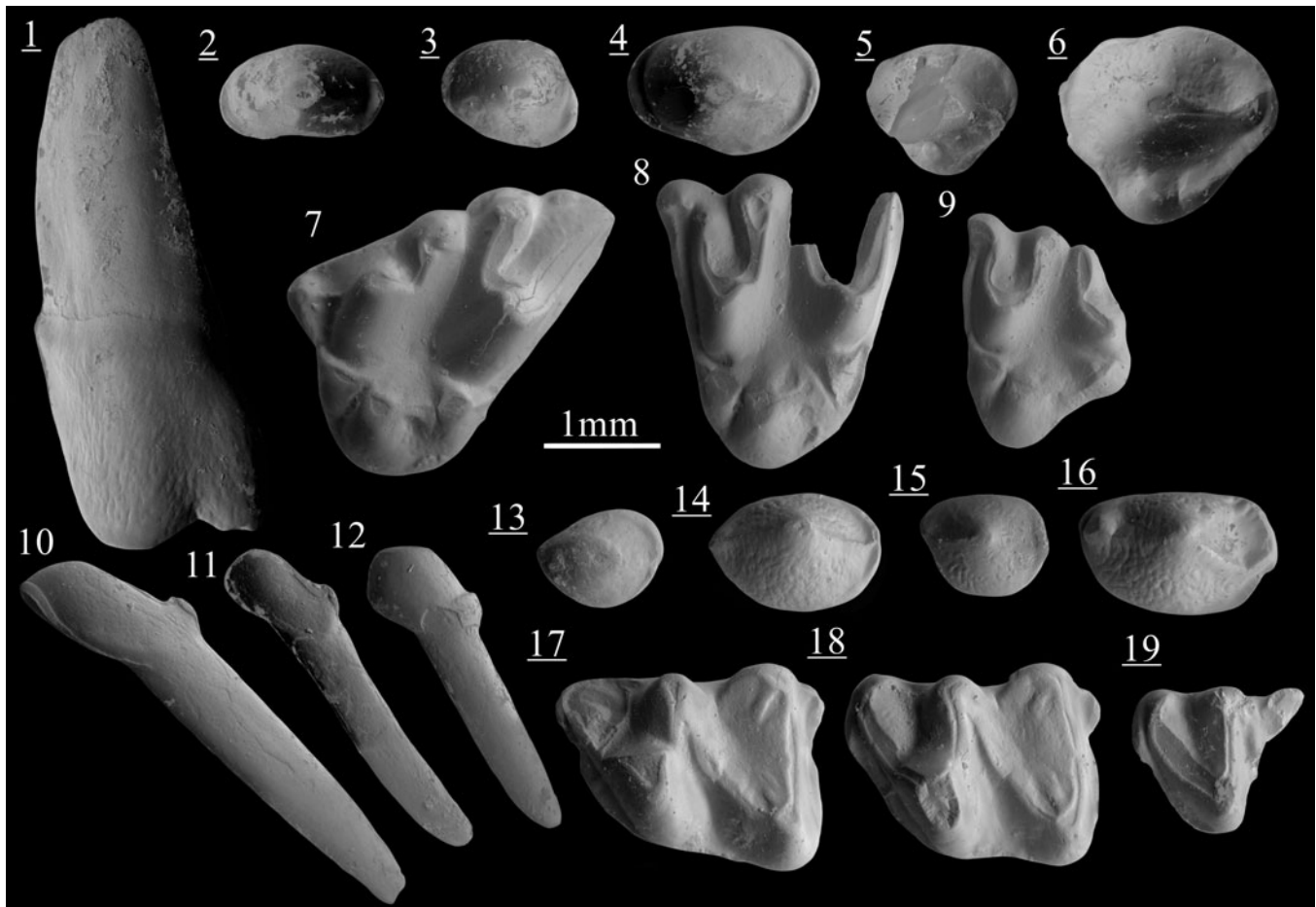


**Figure 3.** Scanning electron photomicrographs of *Archaeodesmana vinea* (Storch, 1978), from Triblavina. (1) I1, TB170231, anterior view; (2) C, TB170258; (3) P1, TB170266; (4) P2, TB170257; (5) P3, TB170218; (6) P4, TB170217; (7) M1, TB170210; (8) M2, TB170211; (9) M3, TB170212; (10) i2, TB170291, labial view; (11) i3, TB170267, labial view; (12) c, TB170278, labial view; (13) p1, TB170289; (14) p2, TB170276; (15) p3 TB170287; (16) p4, TB170286; (17) m1, TB170232; (18) m2, TB170233; (19) m3, TB170294. Images with underlined numbers are reversed.

**Table 3.** Measurements (in mm) of *Archaeodesmana vinea* (Storch, 1978), from Triblavina (MN11) and Krásno (MN11), Slovakia. L = Length; N = number of specimens; W = width; W1 = anterior width; W2 = posterior width.

<i>Archaeodesmana vinea</i> , Triblavina																	
	I1		C		P1		P2		P3		P4		M1		M2		
	L	W	L	W	L	W	L	W	L	W	L	W	L	W	L	W	
N	2	2	1	1	3	3	1	1	1	1	1	1	1	1	1	1	
Min	1.52	1.68			1.15	0.85											
Max	1.59	1.86			1.23	0.91											
Mean			1.42	0.82	1.20	0.87	1.68	1.12	1.27	1.19	1.95	1.73	2.88	2.03	2.11	2.48	
	M3		i2		i3		c		p1		p2		p3		p4		
	L	W	L	W	L	W	L	W	L	W	L	W	L	W	L	W	
N	1	1	1	1	1	1	2	2	1	1	1	1	1	1	1	1	
Min							0.97	0.83									
Max							0.97	0.89									
Mean	1.35	2.00	1.12	0.87	0.98	0.67	0.97	0.86	1.05	0.85	1.46	0.98	1.10	0.88	1.70	1.03	
	m1		m2		m3												
	L	W1	W2	L	W1	W2	W1										
N	1	1	1	1	1	1	1										
Mean	2.27	1.49	1.75	2.20	1.61	1.70	1.22										
<i>Archaeodesmana vinea</i> , Krásno																	
	i2		c		p1		p2		p3		m1		m3				
	L	W	L	W	L	W	L	W	L	W	W1	W2	W1	W2			
N	1	1	2	2	1	1	1	1	2	2	2	1	1				
Min			0.93	0.73					1.15	0.89	1.40						
Max			1.03	0.76					1.21	0.92	1.43						
Mean	1.26	1.07	0.98	0.75	0.87	0.63	1.50	1.12	1.18	0.91	1.42	1.68	1.16				

anterior root insertion is high. The labial flank of the high crown is more convex than the mesial one. Posteromesially a talon is found, surrounded by a thin cingulid connected to the posterior cusplid. The i3 has an asymmetrical outline. From the compressed cusplid descends a mesial slope. A low, longitudinal posterior crest is present. A posterior cingulid is also present, slightly more developed in its most lingual part. The lower canine is a small, rounded tooth that has a more symmetrical outline than the i3. The cusplid is conical and only bears a thin central crest hardly reaching the posterior border. A posterior cingulid is present, more developed on the lingual side.

The p1 is ellipsoidal. It has a pointy anterior border and a straight posterior margin. The only cusplid is in an anteromedial position. A short posterolingual cingulid is distinguishable. The p1 has two distinct roots. The p2 is a big, ovoid tooth with a strong cusplid. A thin crest extends anteriorly and reaches a small pointy bulge. Similarly, a posterior crest reaches the posterior border of the tooth. A posterior cingulid is present. The surface of the tooth is rough (Fig. 3.14). The p3 is a small, rounded tooth with one cusplid. Short centrocrists are present on both the anterior and the posterior side. There is a very reduced posterior cingulid. As on p2, the surface is rough (Fig. 3.15). The p4 is a well-molarized tooth. The protoconid is situated in an anterior position and is connected to a small paraconid by a thin crest. A very weak metaconid is distinguishable on the posterolingual face of the protoconid. A strong crest descends from the posterolabial part of the protoconid and extends transversely, reaching a weak hypoconid. A postcrisid is present, connecting the hypoconid to a hardly distinguishable bulge (entoconid). A posterior cingulid is present, with an especially broad labial part. As in p2 and p3, this tooth has a rough surface (Fig. 3.16).

The m1 has a narrow trigonid. The high protoconid is connected to the metaconid by a blunt protolophid. The entoconid is strong with a high and short entocristid. It is connected to the hypoconid by a thin postcrisid. The hypoconid is weakly developed. A small ridge between the postcrisid and the oblique cristid is present, ending before the wide talonid basin. The oblique cristid is connected to the labial base of the metaconid. The entostylid is robust and connected to a short posterior cingulid. The anterior cingulid is wide but becomes narrower near the paraconid crest. The labial and posterior cingula are well developed. The m2 has a structure similar to the m1 (Fig. 3.17 vs Fig. 3.18). It differs by the broader trigonid, the slightly more compressed paraconid, and the oblique cristid ending more lingually. Only a trigonid of m3 is preserved. It differs from the m1 and m2 by the smaller size, the more curved paraconid crest, a protoconid in a less-anterior position, an oblique cristid clearly connected to the metaconid, and a narrower anterior cingulid.

**Material.**—Pezinok (*Archaeodesmana* cf. *A. vinea*): one P3, one p1 (L = 1.00, W = 0.79).

Triblavina (*A. vinea*): two I1, one C, three P1, one P2, one P3, one P4, one M1, one M2, one M3, one i2, one i3, two c, one p1, one p2, one p3, one p4, one m1, one m2, one m3. Measurements are provided in Table 3.

Krásno (*A. vinea*): one P2, one i2, two c, one p1, one p2, two p3, two m1, one fragment of m1–m2, one fragment of m3. Measurements are provided in Table 3.

**Remarks.**—*Archaeodesmana vinea* is a frequently identified species in the Vallesian and early Turolian of Central Europe (Rümke, 1985; Fejfar and Sabol, 2005; Ziegler, 2006a). Because desmans are conservative in shape, they are mostly identified based on morphometric data, mainly the size proportion of the premolars (Rümke, 1985). Despite that the dental elements of *A. vinea* are relatively homogeneous in size, they display morphological variation in time. Typically, the Vallesian-aged P2 and P3 are double-rooted, whereas Turolian-aged P2 and P3 are triple-rooted (Ziegler, 2006a). Triblavina is an exception as the P2 and P3 still display two roots, whereas this locality is correlated to the lowermost MN11 (Joniak and Šujan, 2020; Joniak et al., 2020). The presence of two roots in *A. vinea* from Triblavina is in line with this locality being older than Eichkogel and Kohfidisch.

The *Archaeodesmana* species from the MN10 of Schernham has been identified as *Archaeodesmana* aff. *A. vinea* by Ziegler (2006a), based on several differences. Even though some of the differences (metaconid on p4, number of roots in P2 and P3) might be attributable to variability and temporal evolution, the very peculiar size ratios of the lower premolars, the large P2, and the overall slenderness of the dental elements make the species from Schernham clearly distinct from other Late Miocene findings. In particular, the p1 of *Archaeodesmana* aff. *A. vinea* is longer than in any other species of *Archaeodesmana*. Additionally, the p1 has significantly larger dimensions than the canine, which is atypical in desmans. The material from Schernham includes mandibles with p1 and canine in position, reducing the possibility of misidentification. Ziegler also separated the measurements of the specimens with uncertain identification (Ziegler, 2006a; Table 5). This supports that the material from Schernham belongs to a new species that evolved in parallel with *Archaeodesmana vinea*.

#### *Archaeodesmana dissona* new species

Figure 4; Table 4

**Holotype.**—Right p2 (L = 1.93, W = 1.16), SG1980027, Šalgovce 5, Slovakia (Fig. 4.14).

**Paratypes.**—From SG1980020 to SG1980054 (excluding SG1980027 = holotype): one P1, one P2, three P3, one fragment of M1, two i1, four i2, three i3, three c, two p1, four p2, two p3, three p4, two fragments of m1, one fragment of m2, one fragment of m3, one posterior fragment of humerus (Ltt = 3.31, Lpt = 2.90, Wcf ≈ 3.26, MDD = 1.41, MDD ref = 1.40). Dental measurements are provided in Table 4.

**Diagnosis.**—Species of *Archaeodesmana* differing from all Desmanini by the following combination of characters: medium size; two-rooted P1; large P2 similar in size to p2; reduced parastyle and accessory cusp on M1; i1 with “a” morphotype (sensu Rümke, 1985); large cingulids on i2; one-rooted p1; high p2/p3 ratio (around 1.45); p2 longer than p4; paraconid distinct on p3, variable on p2; lack of metaconid on p4.

**Differential diagnosis.**—*Archaeodesmana dissona* n. sp. differs from all *Archaeodesmana* species except *A. baetica* by the

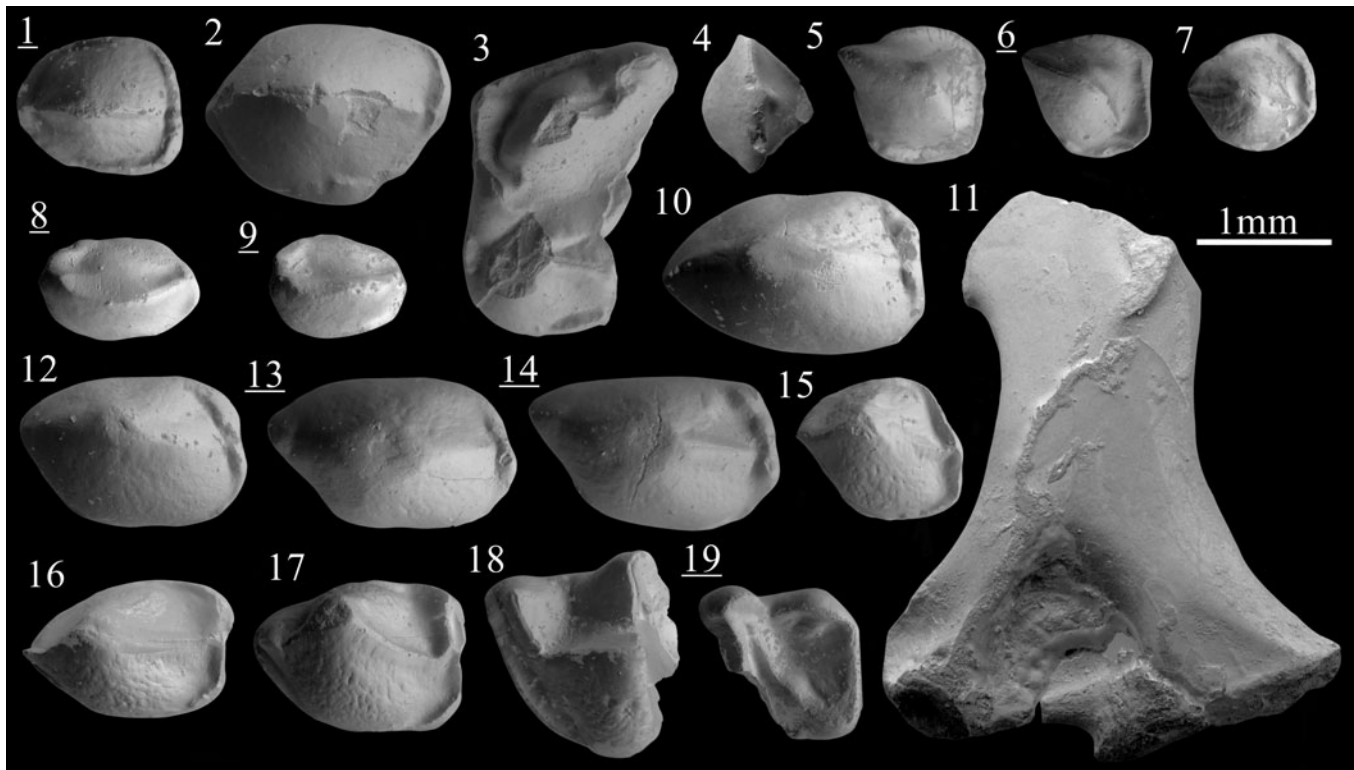


**Figure 4.** Scanning electron photomicrographs of *Archaeodesmana dissona* n. sp. from Šalgovce 5. (1) P1, SG1980040 (paratype); (2) P2, SG1980022 (paratype); (3) M1, SG1980028 (paratype); (4) i1, SG1980042 (paratype); (5) i2, SG1980041 (paratype); (6) i3, SG1980038 (paratype); (7) c, SG1980047 (paratype); (8) p1, SG1980044 (paratype); (9) p1, SG1980045 (paratype); (10) p2, SG1980021 (paratype); (11) humerus, SG1980056, posterior view; (12) p2, SG1980025 (paratype); (13) p2, SG1980026 (paratype); (14) p2, SG1980027 (holotype); (15) p3, SG1980030 (paratype); (16) p4, SG1980031 (paratype); (17) p4, SG1980033 (paratype); (18) m1, SG1980034 (paratype); (19) m3, SG1980037 (paratype). Images with underlined numbers are reversed.

significantly larger dimensions of its p2 (Fig. 5), resulting in much stronger Lp2/Lp3 and Lp2/Lp4 ratios (Table 5); from all *Archaeodesmana* species except *A. major* by the massive P2; from all *Archaeodesmana* species except *A. turolense*, *A. getica*, and *A. acies* by the presence of a paraconid on p3 and p4; from *A. vinea*, *A. adroveri*, *A. turolense*, *A. pontica*, and *A. elvirae* by its single-rooted p1; from *A. baetica* by its significantly smaller p4 and smaller, lower canine (Fig. 5) resulting in a much higher Lp2/Lp4 ratio (Table 5), and the presence of a double-rooted P1.

**Occurrence.**—Šalgovce 5, Topoľčany district, Nitra Region (Slovakia), Danube basin. Correlated to middle Turolian, MN12.

**Description.**—The P1 is a robust, ovoid, and two-rooted premolar. The main cusp is laterally compressed. Straight anterior and posterior ridges start from this cusp and reach the anterior and posterior margin, respectively. A continuous cingulum is present, narrower on the lingual and labial sides. The P2 is an ovoid premolar almost entirely occupied by a conical paracone in central position. A thin posterior ridge is present between the cusp and the posterior cingulum. A weak and low bulge is found at the most-lingual flank of the cusp. A narrow anterior cingulum is present. The P3 is smaller than the P2 but they share a similar labial area. Extending from the paracone, two ridges (anterior and posterior) are distinguishable. A distinct bulge is attached on the lingual flank. This bulge is connected to the lingual cingulum by a

**Table 4.** Measurements (in mm) of *Archaeodesmana dissona* n. sp. from Šalgovce 5 (MN12), Slovakia. L = Length; N = number of specimens; W = width; W1 = anterior width; W2 = posterior width.

	P1		P2		P3		i1		i2		i3		c	
	L	W	L	W	L	W	L	W	L	W	L	W	L	W
N	1	1	1	1	3	3	2	2	2	2	3	3	3	3
Min					1.42	1.05	0.75	0.91	0.85	1.10	0.93	0.83	1.00	0.70
Max					1.48	1.15	0.81	1.05	1.02	1.27	0.99	1.07	1.05	0.86
Mean	1.20	0.99	1.85	1.39	1.45	1.10	0.78	0.98	0.89	1.18	0.96	0.92	1.03	0.80
	p1		p2		p3		p4		m1		m2		m3	
	L	W	L	W	L	W	L	W	W1	W2	W2	W2	W2	W2
N	2	2	4	4	3	2	3	3	1	1	1	1	1	1
Min	1.05	0.75	1.74	1.12	1.28	1.02	1.59	1.06						
Max	1.13	0.77	1.99	1.22	1.34	1.06	1.59	1.11						
Mean	1.09	0.76	1.89	1.16	1.30	1.04	1.59	1.09	1.49	1.51	1.08			

**Table 5.** Main morphological and morphometrical differences between *Archaeodesmana* species. Data according to Rümke (1985), Dahlmann (2001), Martín-Suárez et al. (2001), Ziegler (2005, 2006a), Minwer-Barakat et al. (2008) and this paper.

Species	Locality	MN zone	Lc	Lp1	Lp2	Lp3	Lp4	Lm1	Lp2/Lp3	Lp2/Lp4	Morphology of I1	P1, number of roots	Parastyle extension on M1	Cingulid on i2	p1, number of roots	Distinct paraconid on p2	Distinct paraconid on p3	Distinct metaconid on p4
<i>A. primigenia</i>	Rudabánya	9	1.18	1.32	1.45	1.23	1.52	2.38	0.97	0.83			projected	reduced	2	no	no	yes
<i>A. aff. A. vinea</i>	Schernham	10	0.97	1.05	1.46	1.10	1.70	2.27	1.33	0.86	AW		reduced	2	no	no	yes	
<i>A. vinea</i>	Triblavina	11	0.90	0.90	1.45	1.14	1.63	2.33	1.27	0.89	AW		projected	2	no	no	no	
<i>A. vinea</i>	Dorn—Dürkheim	11	0.99	0.99	1.44	1.15	1.60	2.40	1.25	0.90	AW		projected	2	no	no	yes	
<i>A. vinea</i>	Kohfidisch	11	1.03	1.09	1.89	1.30	1.59	1.45	1.19	0.91	AW	2	reduced	1	variable	yes	no	
<i>A. dissosa n. sp.</i>	Salgotve 5	12	1.10	0.86	1.60	1.41	1.82	2.51	1.13	0.88	AW	2	projected	2	yes	yes	no	
<i>A. adroveri</i>	Aljezar B	12	1.17	1.52	1.31	1.63	2.47	1.16	0.93	0.93	AW	2	projected	2	yes	variable	yes	
<i>A. turoloense</i>	Masada del valle 2	12	1.16	1.00	1.51	1.33	1.65	2.45	1.14	0.92	AW	2	reduced	2	yes	yes	yes	
<i>A. turoloense</i>	Cubla	12	0.92	0.92	1.17	1.60	1.42	1.73	2.63	1.13	AW	2	reduced	1	variable	yes	yes	
<i>A. luteyni</i>	Villalba Baja 1	13	1.16	1.15	1.64						AW	2		2			no	
<i>A. major</i>	Masada del valle 7	13	1.16	0.97	1.48	1.34	1.62	2.37	1.10	0.91	AW	2		2	yes	yes	yes	
<i>A. pontica</i>	Polgárdi	13	1.07	0.91	1.44	1.24	1.58	2.27	1.16	0.91	AW	2		1	yes	variable	yes	
<i>A. getica</i>	Maramena	14	1.22	0.97	2.03	1.43	2.18	2.63	1.42	0.93	AW	1	reduced	1	no	no	no	
<i>A. getica</i>	Kardia	13/14	1.00	0.95	1.32	1.40	1.66	2.43	0.94	0.80	AN	2		1	yes	yes	no	
<i>A. baetica</i>	Purcal 4	14	1.08	0.98	1.40	1.37	1.63	2.85	1.02	0.86	AN	2		1	yes	yes	variable	
<i>A. bifida</i>	Dinar—Akçaköy	15	0.97	1.37	1.26	1.67	2.61	1.09	0.82	0.82	AW	2	reduced	2	no	no	yes	
<i>A. acies</i>	Wölfersheim	15	1.19	1.03	1.49	1.41	1.68	2.52	1.06	0.89	AW	2	projected	1	variable	yes	no	
<i>A. elvrae</i>	Tollo de Chiclana-1	15	1.20	0.88	1.44	1.45	1.73	2.49	0.83	0.83	AW	2	projected	1	no	no	no	
<i>A. brailloni</i>	Sète	16																
<i>A. brailloni</i>	Escorihuela	16																

thin and curved crest. It leads to a slight enlargement of the lingual area. The anterior cingulum shows a thin crest at its margin, barely joining the lingual cingulum.

Only an anterior fragment of M1 has been discovered so far (Fig. 4.3). The paracone is moderately compressed and is connected by a postparacrista to a conical mesostyle. The height of the anterior mesostyle is almost reaching the height of the paracone. The postparacrista is curved. The parastyle is isolated from the paracone and does not create an extension on the anterior margin. It is connected to a labial cingulum ending below the anterior mesostyle, and to an anterior cingulum connected to the well-developed protoconule. A short and thin connection is found between the protoconule and the paracone. A deep valley separates the protoconule from the protocone lingually. On the posterior flank of the protocone a short and straight crest is attached, ending as a blade-like accessory cusp. Broad cingulums are found between the protocone and the protoconule and posteriorly to the protocone.

The i1 has a large chisel-shape crown. The posterior side presents a low talonid resulting in a concave face. A distinct central ridge is present on the posterior flank. The i1 corresponds thus to the “a” morphotype (sensu Rümke, 1985; Fig. 4.4). The i2 is an asymmetrical tooth. Its occlusal outline is quadrangular. The cuspid has a slight anterolingual/posterolabial orientation. Its external flank is slightly concave. An oblique posterior ridge extends from the blade-like apex and ends as a minute tip on the posterolabial margin. The inner cingulid is stronger than the narrow external cingulid. The former extends from the posterior tip of the cuspid as a curve until reaching the higher anterior border of the tooth, where it joins the posterior cristid. The i3 is a small subtriangular tooth bearing one main cuspid in anterior position, from which extends a short anterior crest. An oblique posterior crest connects the cuspid to the posterolabial border. The lower canine is a small ovoid tooth similar to the i3. It differs from the i3 by the more rounded outline, the straighter posterior crest, and the more conical aspect of the cuspid.

The p1 is an ellipsoid premolar with a single, robust root. The cuspid is included in a central ridge extending from the anterior border and reaching the posterior border as a slightly curved crest. The labial side is convex and the lingual side only slightly concave. A barely visible posterior cingulid is present. The p2 is a massive, ellipsoid tooth with two divergent roots. The cuspid is laterally compressed. The anterior end is pointy in occlusal view and presents a distinct shoulder in two out of four specimens. A posterior crest extends from the cuspid and reaches the large and straight cingulid. A narrow cingulid is present all along the labial side. The p3 has a rounded outline and a conical cuspid. A short ridge connects its tip to a minute anterior bulge (paraconid), in a slightly lingual position. The posterior crest is connected to the posterior cingulid. An extremely narrow cingulid is found on the labial side of the tooth. The lingual cingulid is broader and connects the posterior cingulid to the base of the anterior bulge. This creates an asymmetry in which the lingual length is longer than the labial one. The surface of the tooth is slightly rough, as in p3 (Fig. 4.15). The p4 is a double-rooted tooth with a sturdy and conical protoconid. The low paraconid is connected to the protoconid by a thin central ridge. There is no distinguishable metaconid. A crest extends from the posterior part of the protoconid and

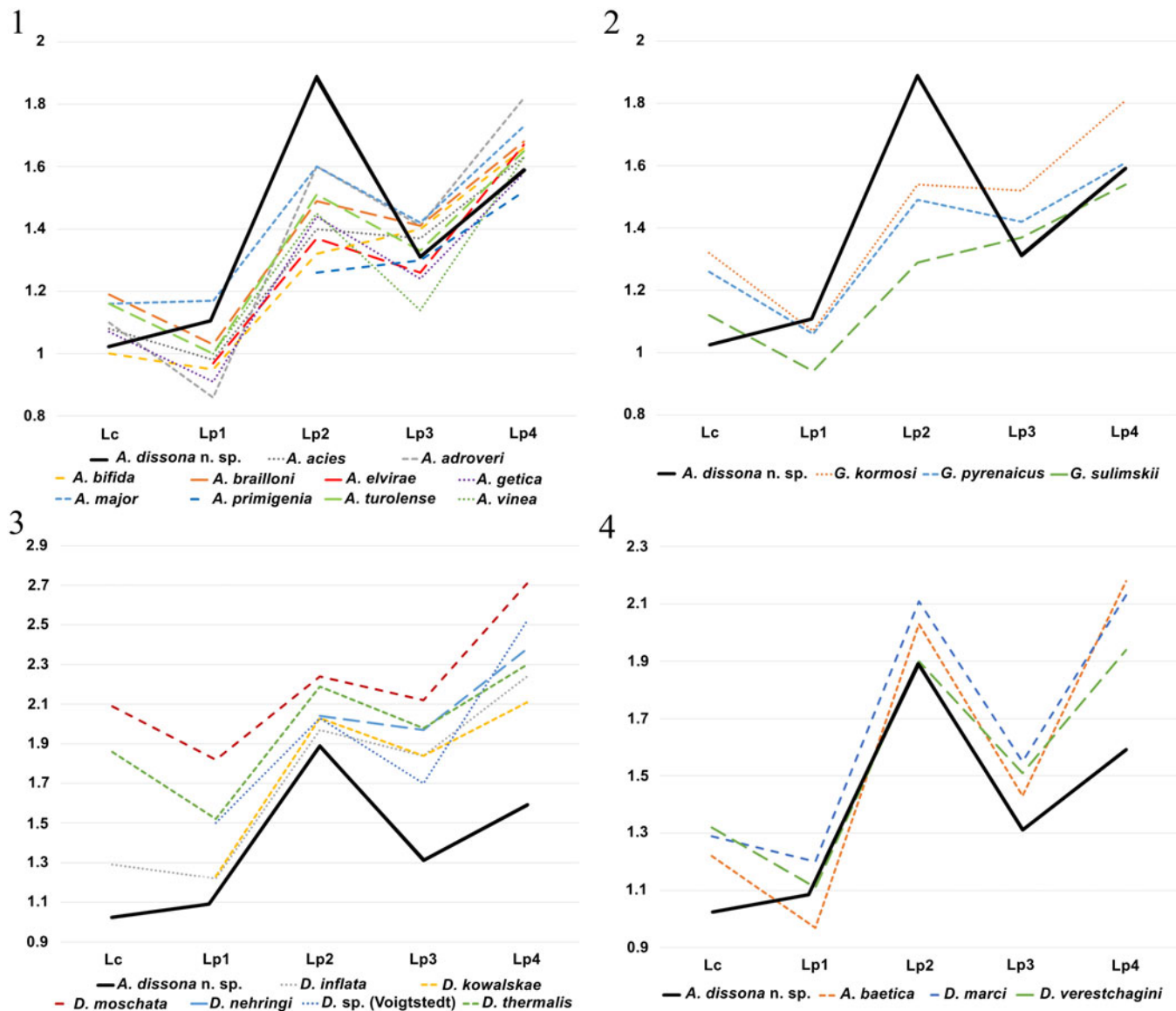


**Figure 5.** Length diagram of the c–p4 of *Archaeodesmana dissona* n. sp. compared to (1) *Archaeodesmana* species; (2) *Galemys* species; (3) *Desmana* species; (4) *A. baetica*, *D. marci*, and *D. verestchagini*. Based on Rümke (1985), Dahlmann (2001), Martín-Suárez et al. (2001), Ziegler (2005, 2006a), Minwer-Barakat et al. (2008, 2020).

turns lingually at the posterior border of the premolar before joining a posterolingual bulge. The posterolabial border possesses a narrow cingulid. A short anterolabial cingulid is present. The surface of the p4 is slightly rough (Fig. 4.16, 4.17).

The trigonid of m1 is slightly laterally compressed. The protoconid is a high subtriangular cuspid connected to a pointy paraconid by a sharply bent paralophid. The metaconid is subtriangular and higher than the paraconid. The oblique cristid is connected to the posterolabial side of the metaconid. The hypoconid is low. The anterior cingulid is broad and continuous. The m2 shares numerous common features with the m1. It differs by its smaller size, the more anteroposteriorly compressed and wider trigonid, and the slightly lower paraconid and hypoconid. The trigonid of m3 is anteroposteriorly compressed. The paraconid is included in the paralophid. The conical metaconid and the trifaced protoconid have the

same height. The talonid of m3 is wider than long. The low hypoconid is connected to the posterior base of the conical metaconid by the oblique cristid. The entoconid is laterally compressed and leads to a short entocristid stopped by a notch. The postcristid is straight.

The posterior fragment of humerus shows clear desmanine affinities (Fig. 4.11). The diaphysis is narrow but with a relatively low pectoral tubercle and short tuberculum teres. The capitulum area is large. A noticeable groove is present between the stout trochlea and the fossa for the musculus flexor digitorum ligament. The entepicondyle is broken; it is thin on its anterior-most part. It continues as a thicker ridge on the posterior view, stopping at the central part of the diaphysis. The fossa supratrochlearis is broad, deep, and has a rounded shape. The fossa olecrani is shallower and more compressed. The foramen entepicondylaris is elongate.

*Etymology*.—From the Latin “dissonus, -a, -um”: dissonant, discordant. In reference to the unusual dental ratio of the premolars.

*Remarks*.—The identification of a single species of *Archaeodesmana* in the material from Šalgovce 5 is supported by the homogeneity of the lower dentition. Overall, the dental pattern of *Archaeodesmana dissona* n. sp. is similar to Turolian species such as *A. getica*, but the combination of one-rooted p1 and extraordinarily robust p2 are enough to differentiate our material from any Late Miocene species (Fig. 5). The single exception is *A. baetica*, which, however, shows a much stouter and larger p4 whereas our species retained a p4 with ancestral shape and dimensions.

The ratio of the lower premolars (Fig. 5) highlights the strong similarities between our species and *Archaeodesmana baetica* (MN13/14), *Desmana marci* Minwer-Barakat et al., 2020 (MN14), and *Desmana verestchagini* (Topachevski, 1961) (MN14). These three species represent *Archaeodesmana–Desmana* transitional forms because each species acquired new features typical of *Desmana* (see Minwer-Barakat et al., 2020), strongly anchoring the origin of *Desmana* on the Iberian Peninsula. The found similarities likely correspond to convergent evolution. Similarly, the root reduction of p1 was previously attested only from the MN13 with *A. getica*. This feature is not present in the third late Turolian species from Central Europe, *A. pontica*. The scarcity of the Central European fossil record greatly limits phylogenetic discussion. Nevertheless, the distinctions found between *A. getica*, *A. pontica*, and *A. dissona* n. sp. support the presence of several Central European lineages evolving in parallel during the Turolian. Additionally, the early acquisition of convergent features in *A. dissona* n. sp. makes this species a good example of mosaic evolution.

A humerus is tentatively attributed to *Archaeodesmana dissona* n. sp. on the grounds of its resemblance with the humeri of *A. baetica* (see Martín-Suárez et al., 2001) and *A. getica* (see Terzea, 1980; Rümke, 1985). Because Šalgovce 5 also contains a second desmanine whose humerus is unknown, we refrain from providing a firm attribution.

Genus *Gerhardstorchia* Dahlmann and Doğan, 2011

*Type species*.—*Gerhardstorchia wedrevis* (Dahlmann, 2001).

*Other referred species*.—*Gerhardstorchia quinquecuspidata* (Mayr and Fahlbusch, 1975); *G. biradicata* (Ziegler, 2006a); *G. meszaroshi* (Sabol, 2005).

*Diagnosis*.—See Dahlmann (2001, p. 35).

*Occurrence*.—This genus is identified from MN6 to MN15 of Central Europe (Dahlmann, 2001; Sabol, 2005; Ziegler, 2006b).

*Remarks*.—Dahlmann and Doğan (2011) erected *Gerhardstorchia* as nomen novum for the genus *Storchia* Dahlmann, 2001, preoccupied by *Storchia* Oudemans, 1923.

*Gerhardstorchia biradicata* (Ziegler, 2006)  
Figure 6.1–6.5

*Holotype*.—Left fragment of mandible with p1–m2, NHMV 2004z0190/0001, Schernham, Austria (Ziegler, 2006a).

*Diagnosis*.—See Ziegler (2006a, p. 118).

*Occurrence*.—From MN9 to MN11 of Austria (Ziegler, 2006a), and MN9 of Slovakia (this paper).

*Description*.—The I1 is a massive tooth with a high crown that is oblique in occlusal view. A ridge starts from the most external crest, extending all along the posterior side of the tooth and reaching a protruding posterolabial bulge. A hardly visible ridge is also present on the other side of the tooth. A narrow posterior cingulum is present.

The c is a compressed, one-rooted tooth with a single, laterally compressed cuspid in an anterior position. A crest connects the tip of the cuspid to the anterior margin. A posterior crest is also present but does not reach the posterior border of the tooth. A narrow cingulid is found along the posterior and lingual sides.

The p1 has a single, ellipsoid root. The protoconid is pointy and in anterior position. A short, low, and curved anterior crest is present. The posterior crest is strong but does not reach the posterior margin. The posterior and lingual sides bear a cingulid. On the labial side, a hardly distinguishable cingulid is found.

The m2 is relatively stout and elongated (Fig. 6.4). The paraconid is the lowest cuspid of the tooth. The protoconid is high and triangular in cross-section. It is separated from the conical metaconid by a distinct protolophid. The trigonid basin is reduced but lingually open. The entoconid is slightly higher than the hypoconid and is connected to it by a low postcrisid. The oblique cristid reaches a distinct metacristid. The entostylid is attached to the wall of the entoconid. The anterior cingulid is large, especially below the paraconid. The m3 has a similar configuration as the m2 but with a longer protolophid and a narrower talonid. The hypoconid is especially low (Fig. 6.5). There is no entostylid.

*Material*.—Studienka E: one I1 (L = 1.32, W = 0.76), two c (L = 1.19, W = 0.61; L = 1.22, W = 0.64), one p1 (L = 1.41, W = 0.58), one m2 (L = 2.37, W1 = 1.34, W2 = 1.45), one m3 (L = 1.38, W1 = 0.86, W2 = 0.70).

*Remarks*.—The massive desman-like I1 is more gracile than in *Archaeodesmana*, *Desmana*, and *Galemys*, and fits perfectly with the genus *Gerhardstorchia* as defined by Dahlmann (2001). The presence of a metacristid on m2 and m3 is found in *Gerhardstorchia biradicata*, already identified in the MN9 and MN10 of the Vienna basin by Ziegler (2006a). After direct comparison, no differences are found with the type material from Schernham.

*Gerhardstorchia* sp.  
Figure 6.6, 6.7.

*Description*.—The P4 is slightly broken (Fig. 6.6). This relatively flat, subtriangular premolar displays a low, conical paracone in a slightly anterior position, connected by two thin ridges to a broad posterior cingulum and a narrower anterior

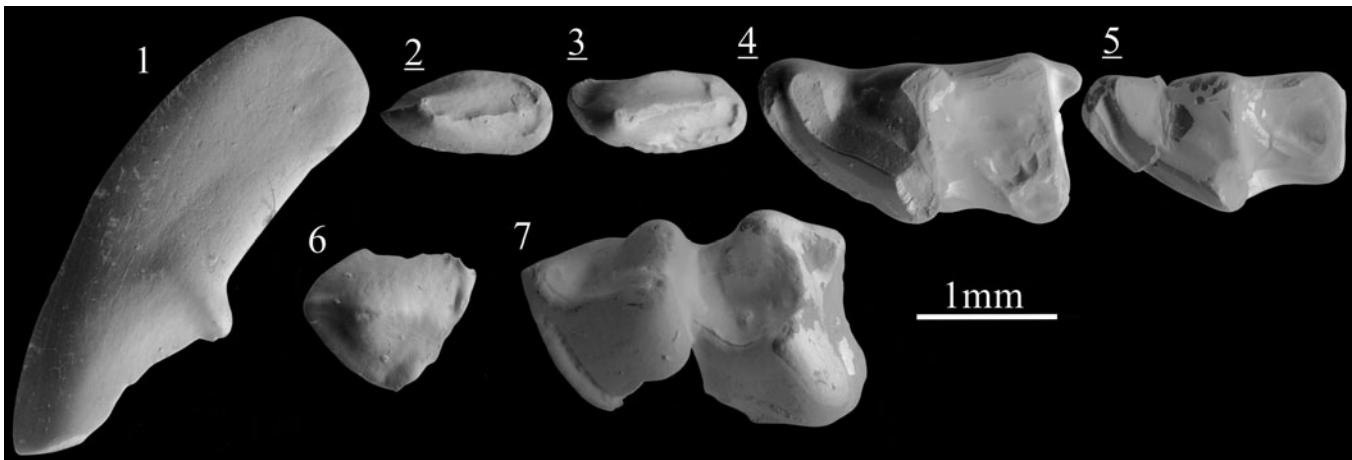


**Figure 6.** Scanning electron photomicrographs of (1–5) *Gerhardstorchia biradicata* (Ziegler, 2006a) from Studienka E and (6, 7) *Gerhardstorchia* sp. (1) I1, ST220043, labial view; (2) c, ST220042; (3) p1, ST220040; (4) m2, ST220044; (5) m3, ST220045; (6) P4, SG1980060; (7) m1, SG1980061. Images with underlined numbers are reversed.

cingulum. A short lingual extension is present, only bearing a small elevation at the most lingual margin.

The single m1 is damaged (Fig. 6.7). The trigonid has a triangular shape and a very reduced configuration. The low paraconid is included in the paralophid, the anteriormost segment of which is short. The conical metaconid is partly attached to the higher protoconid. The talonid displays a low but robust entoconid and hypoconid. The oblique cristid reaches the central part of the trigonid wall. The entostylid corresponds to a bulge attached behind the entoconid. The anterior cingulid is broad whereas the posterior one is narrow.

**Material.**—Šalgovce 5: one broken P4, one broken m1 (L = 2.30, W2 = 1.46).

**Remarks.**—The stout m1 with a central paraconid is distinct from *Archaeodesmana* and *Mygalinia hungarica* (Kormos, 1913). The overall morphology of this element reveals strong affinities with *Gerhardstorchia*. The m1 is broader than in *G. biradicata* and *Gerhardstorchia* sp. from Dorn-Dürkheim (Dahlmann, 2001). It is similar in size and shape with the MN9 *G. quinquecuspidata* from Hammerschmiede (Mayr and Fahlbusch, 1975). The persistence of the latter species until the MN12 is rather unlikely. At least, the *Gerhardstorchia* species from Šalgovce 5 fill the temporal gap between Late Miocene and Pliocene occurrences of the genus. It also tends to contradict the idea of a slendering of the dentition in *Gerhardstorchia* over time (Dahlmann, 2001), as already discussed by Ziegler (2006a).

Tribe Scalopini Trouessart, 1879  
*Proscapanus* Gaillard, 1899

**Type species.**—*Proscapanus sansaniensis* (Lartet, 1851).

**Other referred species.**—*Proscapanus lehmanni* (Gibert, 1975); *P. intercedens* Ziegler, 1985; *P. austriacus* Ziegler, 2006a; *P. minor* Ziegler, 2006a; *P. metastylidus* Rzebik-Kowalska and Lungu, 2009.

**Diagnosis.**—See Gaillard (1899, p. 23).

**Occurrence.**—*Proscapanus* is encountered in Europe from the Early Miocene (MN2) to the Late Miocene (MN10) (Ziegler, 2006a, b; Rzebik-Kowalska and Lungu, 2009; Klietmann et al., 2015). Its presence in China is attested in several Early and Middle Miocene faunas (Tao, 2006; Qiu et al., 2013).

*Proscapanus minor* Ziegler, 2006  
Figure 7.1–7.15; Table 6

**Holotype.**—Right M1, NHMV 2004z0197/0001, Schernham, Austria (Ziegler, 2006a).

**Diagnosis.**—See Ziegler (2006a, p. 128).

**Occurrence.**—MN9 and MN10 of Austria (Ziegler, 2006a), and MN9 of Slovakia (this paper).

**Description.**—The P3 is an elliptical, one-rooted premolar with a cusp in anterior position. The tip of the cusp is slightly laterally compressed. A short anterior crest is distinguishable. The posterior crest is thin and elongated. It joins a broad and rounded cingulum that is lacking beneath the anterior flank of the cusp. The P4 is a triangular, three-rooted premolar bearing a conical paracone situated in an anterior position. The parastyle is weak. It is bent in one specimen out of four. The metastyle is weakly to moderately connected to the straight labial crest. From the posterolabial margin (from the metastyle when present) extends a low lingual cingulum connected to a slightly laterally compressed protocone. The anteriormost base of the protocone is connected to the parastyle by a very reduced anterior cingulum.

The three-rooted M1 has a stretched outline (Fig. 7.2). The metacone is a strong, elongated cusp connected to an almost straight postmetacrista. The premetacrista is connected to a mesostyle whose height is similar to that of the metastyle. The two mesostyles are superficially divided. Whereas the posterior mesostyle only has a pointy tip, a short, descending crest is

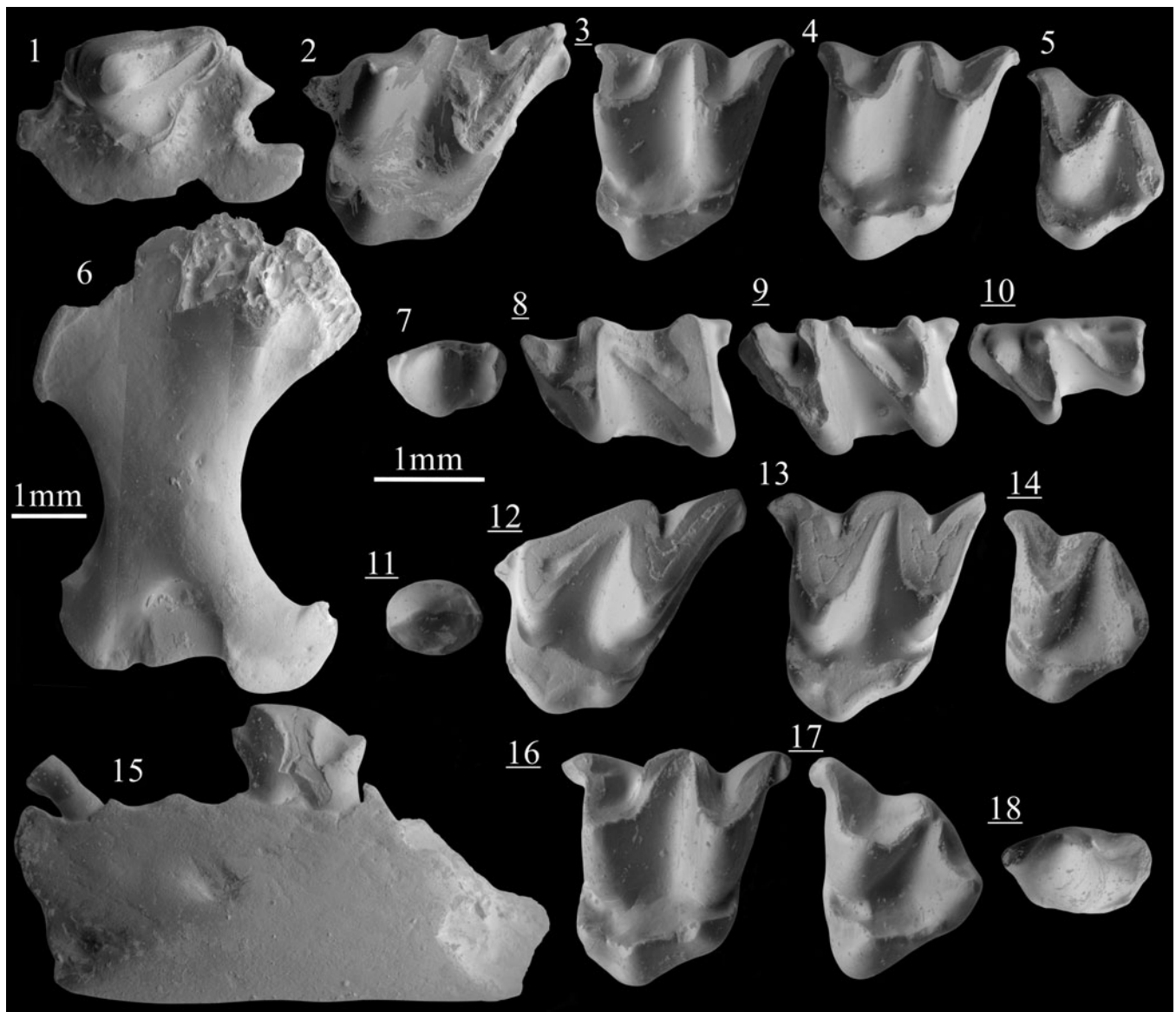


**Figure 7.** Scanning electron photomicrographs of (1–15) *Proscapanus minor* Ziegler, 2006a, from (1–10) Borský Svätý Jur and (11–15) Studienka A; and (16–18) *P. austriacus* Ziegler, 2006a, from Studienka A. (1) P4, BJ213376; (2) M1, BJ213350; (3) M2, BJ213358; (4) M2, BJ213365; (5) M3, BJ213382; (6) humerus, BJ213443, posterior view; (7) p4, BJ213389; (8) m1, BJ213395; (9) m2, BJ213413; (10) m3, BJ213428; (11) P3, ST214281; (12) M1, ST214250; (13) M2, ST214258; (14) M3, ST214261; (15) mandible with broken p1 and p4, labial view; (16) M2, ST214221; (17) M3, ST214222; (18) P4, ST214223. Images with underlined numbers are reversed.

posteriorly attached to the anterior mesostyle. The paracone is weaker than the metacone. A projected parastyle is attached to its anterior base. The parastyle is connected by a thin preprotoconulecrista to a high protoconule, which is attached to the anterior slope of the protocone. The latter is connected by a narrow ridge to the conical hypocone. From the hypocone starts a short ridge extending along the posterior cingulum, ending below the metastyle as a pointy, projected bulge.

The M2 has three roots and a symmetrical labial aspect (Fig. 7.3, 7.4). Metacone and paracone are high, lingually elongated cusps. The base of the metacone is situated slightly more labially than that of the paracone. Both cusps lead to two adjoining mesostyles. The protoconule is placed more anteriorly than the paracone. It is better separated from the protocone than in

M1, but is still connected to this cusp by a high and narrow crest. The protocone is conical. The hypocone is more labial than the protocone and the protoconule and it has an intermediate height. It is connected to the protocone by a narrow oblique crest. From the posterior base of the hypocone and the anterior base of the protoconule start short crests reaching the posterior and anterior margin of the tooth, respectively.

The M3 is a reduced molar with three roots, the posterior root being almost divided. The metacone is an obliquely compressed cusp with no postmetacrista. The small posterior tip of the mesostyle is sometimes not distinguishable from the curved premetacrista. The anterior mesostyle is slightly higher and stronger than the posterior one. The paracone is in a more lingual position than the metacone. The preparacrista leads to a curved



and unreduced parastyle. The protoconule is small, attached to the base of the paracone and connected to the protocone by a low ridge. The protocone is almost conical and connected to a small hypocone.

Three circular alveoli are found anterior to the p4, interpreted as belonging to the p1, p2, and p3. The coronoid process is high and slightly posteriorly projected. The angular process is only preserved in its anterior part and shows an extended concave surface. The masseteric fossa is as deep as the internal temporal fossa. A broad and low central crest separates the internal temporal fossa from an enlarged mandibular foramen, situated below the posterior tip of the coronoid process. A foramen is found below the root of the p3 and the anterior root of the p4 (Fig. 7.15).

The two-rooted p4 is an elliptical premolar with a bent protoconid in an anterior position. A small projecting and independent paraconid is found at the anterolingual border. A posterolingual swelling extends from the tip of the protoconid until the talonid but is interrupted by a notch. The posterior cingulid encloses the talonid. A cuspule is distinguishable on the lingual part of that cingulid.

The m1 has two roots. The trigonid is narrow. The paraconid is the lowest cuspid of the trigonid, followed by the metaconid. The paralophid and the protolophid are bi-partitioned. The protoconid is situated in a central position and is more anterior than the metaconid. The talonid is larger than the trigonid. The hypoconid is as high as the protoconid. The oblique cristid is connected to a pointy metacristid (six out of eight specimens) or is attached to the trigonid wall near a shorter metacristid (Fig. 7.8). The entoconid has an oval base and is slightly shorter than the metaconid. There is an entocristid in six out of eight specimens. When absent, the talonid basin is open lingually. The entostylid corresponds to a small bulge below the entoconid. The short anterior cingulid (present in six out of seven specimens) is not connected to the narrow labial cingulid. The m2 is similar to the m1, but longer and larger. The trigonid and talonid are of similar width. The m2 shows a stronger metastylid (Fig. 7.9), connected to the base of the metaconid. The talonid basin is always closed by a low entocristid. The anterior cingulid of m2 is broader than in m1. The m3 has two roots, an anteroposteriorly compressed trigonid and a narrow talonid. The paraconid is the lowest cuspid of the trigonid. It is connected by a straight crest to the protoconid. The oblique cristid leads to a low cuspule attached to the metaconid. The entocristid closes the narrow talonid basin. The anterior and labial cingulids are broad.

The humerus (Fig. 7.6) is moderately stout, with a broad pectoral area and a slightly curved diaphysis. The pectoral area is damaged, but a thin transversal ridge is distinguishable. The fossa brachialis consists of a superficial basin. The groove between the greater tuberosity and pectoral crest is large in anterior view but shallow in posterior view. The partially preserved tuberculum teres is slightly curved. It is connected to the pectoral tubercle by a thin pectoral ridge. A second straight ridge reaches the pectoral tubercle. On the posterior side, the capitulum is bulbous and elongated whereas the ectepicondyle is reduced. This creates a strong, transversal extension on the posterior epiphysis. The supratrochlear fossa is short, slightly compressed, and deep. The notch between the trochlea and the insertion fossa for the musculus flexor digitorum ligament is

shallow. The entepicondyle is reduced and does not show any spine but a thin angular rib. The foramen entepicondylaris is enlarged.

*Material.*—Borský Svätý Jur: one P3, four P4, seven M1, 16 M2, 12 M3, six p4, three fragment of mandibles with m1 and m2, 10 m1, 16 m2, 14 m3, one humerus (BJ213443: Ltt = 4.55, Lpt  $\approx$  3.50, Ltm  $\approx$  9.04, Wcf = 4.76, Mdd = 2.40, Mdd ref = 2.34). Dental measurements are provided in Table 6.

Studienka A: one P3, three P4, five M1, three M2, three M3, one fragment of mandible with p4, one p4, six m1, four m2, six m3. Measurements are provided in Table 6.

*Remarks.*—Although the Austrian *Proscapanus* material from Schernham shows a bimodal size distribution, only small-sized specimens are recorded in Richardhof–Wald and Richardhof–Golfplatz, motivating the erection of the small *P. minor* and the bigger *P. austriacus* (see Ziegler, 2006a). As in Schernham, an enlarged morphological and morphometrical variability is found in the material from Studienka A. On the other hand, the material from Borský Svätý Jur is rather intermediate in size between *P. minor* and *P. austriacus* (Fig. 8). The specimens from Borský Svätý Jur do not exhibit the few morphological autapomorphies of *P. austriacus*, supporting their attribution to the ancestral *P. minor*. The gradual acquisition of the divergent, diagnostic peculiarities of both species in MN9 (Fig. 8) highlights the impact of competition in their evolution (see Discussion).

*Proscapanus austriacus* Ziegler, 2006  
Figure 7.16–7.18

*Holotype.*—Left M1, NHMV 2004z0196/0001, Schernham, Austria (Ziegler, 2006a).

*Diagnosis.*—See Ziegler (2006a, p. 124).

*Occurrence.*—MN9 of Moldova (Rzebik-Kowalska and Lungu, 2009) and Slovakia (this paper), and MN10 of Austria (Ziegler, 2006a).

*Description.*—On M2, the paracone is slightly larger than the metacone but has a similar height. The tips of the mesostyles are adjoining. The parastyle is slightly higher than the metastyle. The lingual cusps are well differentiated. The protoconule is laterally compressed and connected to the protocone by a very short crest. The protocone is connected to the base of the pointy hypocone by a straight ridge. Two external ridges start from the hypocone, ending beneath the anterolingual flank of the protocone and the posterolingual flank of the metacone, respectively. The M3 is almost triangular in the occlusal view (Fig. 7.17). The metacone is compressed and without postmetacrista. Its dimensions are clearly smaller than the paracone. The anterior mesostyle is stronger than the posterior one. Their tips are adjoining. The preparacrista leads to a curved and stout parastyle. Between the mesostyles and the parastyle is a distinct mortar-like basin, largely open labially. The protocone is almost conical and connected to a cingulum ending beneath the anterolingual

**Table 6.** Measurements (in mm) of *Proscapanus minor* Ziegler, 2006a, from Borský Svätý Jur (MN9) and Studienka A (MN9), Slovakia. L = Length; N = number of specimens; W = width; W1 = anterior width; W2 = posterior width.

<i>Proscapanus minor</i> , Borský Svätý Jur																
	P4		M1		M2		M3		p4		m1		m2			
	L	W	L	W	L	W	L	W	L	W	L	W1	W2	L	W1	W2
N	4	3	3	1	8	10	6	5	6	6	8	9	10	3	8	9
Min	1.38	1.16	2.07		1.84	1.95	1.18	1.79	0.98	0.60	1.91	0.97	1.15	1.94	1.21	1.16
Max	1.65	1.19	2.21		2.03	2.18	1.31	1.95	1.12	0.67	2.09	1.07	1.32	2.08	1.32	1.38
Mean	1.51	1.17	2.14	2.34	1.90	2.07	1.26	1.81	1.06	0.64	1.95	1.03	1.26	2.03	1.26	1.23
<i>Proscapanus minor</i> , Studienka A																
	P3		P4		M1		M2		M3		p4		m1		m2	
	L	W	L	W	L	W	L	W	L	W	L	W1	W2	W2		
N	1	1	3	3	3	3	2	3	1	2	2	1	4	3		
Min			1.56	2.06	2.15	1.85	2.01			1.71	1.01	0.58		1.21	1.22	
Max			1.61	2.35	2.40	1.94	2.07			1.77	1.24	0.70		1.28	1.37	
Mean	0.86	0.67	1.58	2.21	2.24	1.89	2.04	1.29	1.74	1.13	0.64	1.11	1.24	1.28		
<i>Proscapanus minor</i> , Studienka A (continued)																
	m3		W1		W2											
	L	W	L	W												
N	8	14	11													
Min	1.64	1.02	0.81													
Max	1.89	1.18	0.98													
Mean	1.75	1.08	0.91													

flank of the protocone. The hypocone corresponds to a rib on the angular crest.

The p4 is an elliptical tooth with a massive, conical main cuspid in anterior position. A short anterior crest is found at the anterior flank of this cuspid, turning lingually after reaching the anterior margin. There is no posterior crest. The talonid is broad lingually but narrower labially. The thin cingulid encapsulates a reduced posterolingual basin.

Lower molars are poorly preserved. They do not have a posterior cingulid but a strong entostylid. The trigonid of m2 has a width similar to that of the talonid. The trigonid is compressed and triangular in cross-section. The protoconid is the highest cuspid. The talonid has two well-developed cuspid. The metacristid

and the entocristid are slightly separated. The oblique cristid is attached to the metaconid. The m3 has rather large dimensions. The talonid is strongly compressed whereas the trigonid preserves its triangular occlusal outline. The hypoconid and entocoid are reduced and hardly distinguishable from the postcristid on worn specimens. A thin metacristid connects the base of the metaconid to the base of the entoconid. The posterolabial cingulum is present. The anterior cingulid is prominent.

**Material.**—Studienka A: two M2 (L = 2.11, W = 2.15), one M3 (L = 1.45, W = 2.15), one p4 (L = 1.38, W = 2.03), one m1 (W2 = 1.33), two m2 (W2 = 1.35), two m3 (L = 1.99, W1 = 1.05, W2 = 0.98; W2 = 0.84).

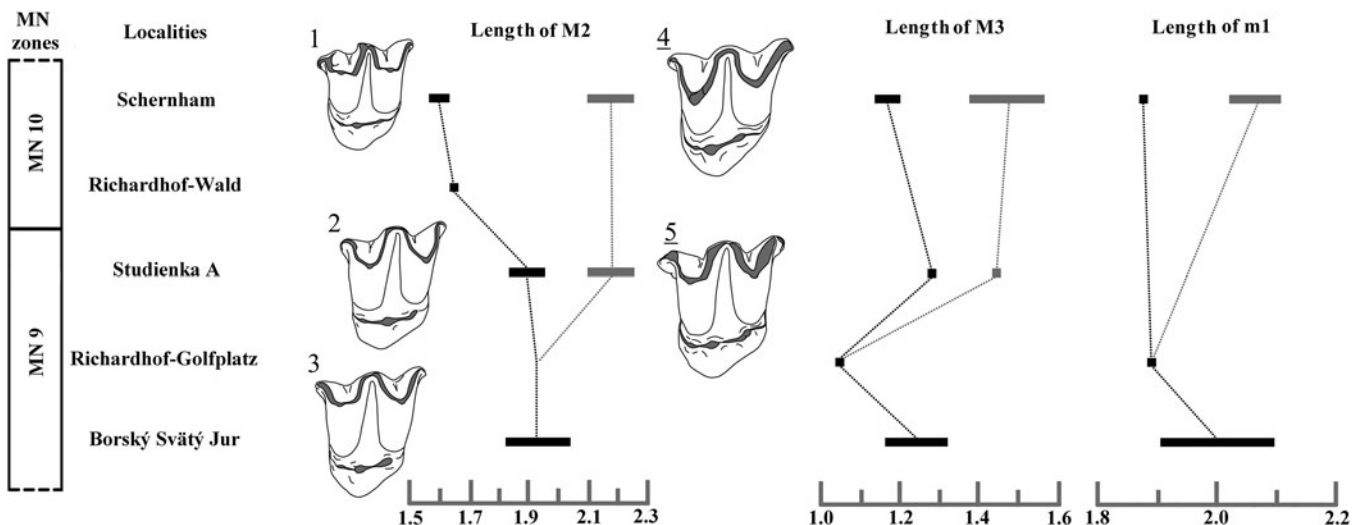


**Figure 8.** Hypothetical reconstruction of the speciation process of *Proscapanus* in the Late Miocene of Austria and Slovakia, showing the length measurement of M2, M3, and m1 of (1–3) *P. minor* Ziegler, 2006a, and (4, 5) *P. austriacus* Ziegler, 2006a. (1) NHMV 2004z0197/0007, Schernham; (2) ST214260; (3) BJ213365; (4) NHMV 2004z0196/0009, Schernham; (5) ST214221.

*Remarks.*—These few specimens already display the diagnostic features acquired by *Proscapanus austriacus*. Namely, the larger size, the better differentiated lingual conules on M1–2 and the reduced cingulid on m1. This indicates that *P. austriacus* emerged during latest MN9 (Fig. 8).

Tribe Talpini Fischer, 1814

*Talpa* Linnaeus, 1758

*Type species.*—*Talpa europaea* Linnaeus, 1758.

*Other referred species.*—*Talpa minuta* de Blainville, 1840; *T. fossilis* Petenyi, 1864; *T. minor* Freudenberg, 1914; *T. gracilis* Kormos, 1930; *T. praeglacialis* Kormos, 1930; *T. vallesensis* Villalta and Crusafont, 1944; *T. gilothi* Storch, 1978; *T. neagui* Radulescu et al., 1989; *T. tenuidentata* Ziegler, 1990. All modern species distinguished by Bannikova et al. (2015) are also included.

*Occurrence.*—*Talpa* is an extant, widely spread Eurasian genus (e.g., Villalta and Crusafont, 1944; Radulescu et al., 1989; Bannikova et al., 2015). Its earliest record is in MN 2 in the locality of Ulm-Westtangente, Germany (Ziegler, 1990).

*Talpa* cf. *T. minuta* de Blainville, 1840

Figure 9.1, 9.2

*Lectotype.*—Right humerus, Sa. 12020 MNHN, Sansan, France (Engesser, 2009).

*Diagnosis.*—See Engesser (2009, p. 44).

*Occurrence.*—MN3 to MN9 of Europe (Ziegler, 1994, 2003; Kälin and Engesser, 2001; Sabol, 2005; Engesser, 2009).

*Description.*—The P4 is a gracile tooth (Fig. 9.1) with a slightly elongated paracone in anterior position. A short anterior extension is attached to the paracone with a hardly distinguishable parastyle. A straight posterocrista extends from the tip of the paracone and reaches the posteriormost margin. The lingual part of the P4 is narrow and bears a strong conical protocone.

The subtriangular M3 has a broken preparacrista. The paracone is subtriangular in cross section whereas the metacone is conical. The mesostyles are not distinguishable from the confluent postparacrista and premetacrista. The lingual area is simplified. From the small protocone, two ridges start: the anterior ends aside the base of the paracone whereas the posterior one reaches the lingual face of the metacone. The only cingulum is found between the mesostyle and the parastyle.

*Material.*—Studienka A: one P4 (L = 1.13, W = 0.87), one M3 (L = 1.12).

*Remarks.*—These two elements are grouped together because of their correspondence with the *Talpa* morphotype. Their sizes coincide with the smallest *Talpa* recorded from the Late Miocene, *Talpa* aff. *T. minuta*, identified in the MN10 and MN11 of Austria (Ziegler, 2006a). This Late Miocene

Austrian species displays a P4 without a protocone, which is a morphological feature not found in *T. minuta* from Sansan. The P4 from Studienka A still preserves this cusp.

Tribe Urotrichini

Urotrichini gen. and sp. indet.

Figure 9.3

*Description.*—The P4 (Fig. 9.3) has a slightly elongated paracone and a small projected parastyle. The lingual extension is narrow and bears a distinct protocone. The M1 is a tiny molar with slightly stretched paracone and metacone. The postparacrista is almost parallel to the labial margin. The mesostyle is not divided on the single worn specimen. The lingual area is weakly developed. The parastyle is projected anteriorly. From the hypocone extends a crest reaching the posterolingual base of the metacone.

The p4 is a gracile, two-rooted premolar with a main conical cuspid in anterior position. The base of the protoconid is slightly extended anteriorly. A ridge extends from the posterolingual tip of the protoconid to the posterior margin before joining a hardly visible cingulid.

*Material.*—Triblavina: one fragment of P4, one fragment of M1.

Krásno: one p4 (L = 0.95, W = 0.50).

*Remarks.*—These findings are lumped together considering their very small size and similar evolutionary stage. The M1 of *Talpa minuta* displays a more oblique postparacrista (Engesser, 2009) and Turolian affinis forms have a more reduced P4 (Ziegler, 2006a). The configuration of P4 and p4 and the slight obliquity of M1 are consistent with a small urotrichine species. They are tentatively attributed to the latter tribe.

Subfamily Incertae sedis

Genus *Desmanodon* Engesser, 1980

*Type species.*—*Desmanodon major* Engesser, 1980.

*Other referred species.*—*Desmanodon minor* Engesser, 1980; *D. antiquus* Ziegler, 1985; *D. daamsi* van den Hoek Ostende, 1997; *D. ziegleri* van den Hoek Ostende, 1997; *D. burkarti* van den Hoek Ostende, 1997; *D. crocheti* Prieto, 2010; *D. fluegeli* Prieto et al., 2010; *D. larsi* Furió et al., 2014.

*Diagnosis.*—See Engesser (1980, p. 116).

*Occurrence.*—*Desmanodon* is encountered from the Early to Late Miocene of Anatolia (Engesser, 1980; van den Hoek Ostende, 1997; Furió et al., 2014; Bilgin et al., 2019) and from the Early to early Late Miocene of Europe (van den Hoek Ostende, 1997; Ziegler, 2003; Prieto, 2010; Prieto et al., 2010, 2015; this paper).

*Desmanodon* cf. *D. fluegeli* Prieto et al., 2010

Figure 9.4–9.9

*Holotype.*—Fragment of right mandible with c, p3–m3, LMJG 204.164, Gratkorn, Austria (Prieto et al., 2010).

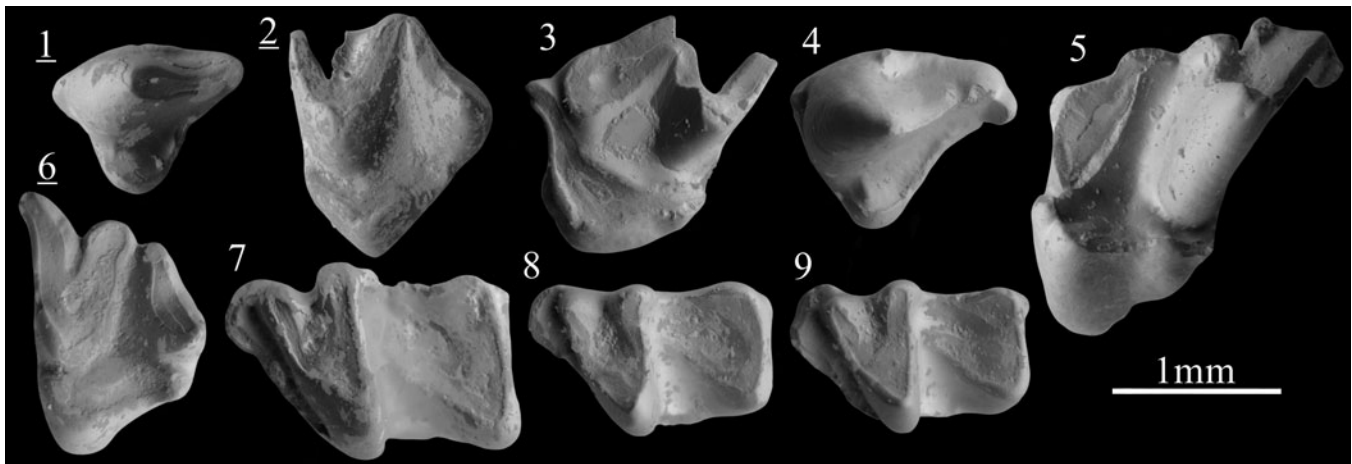


**Figure 9.** Scanning electron photomicrographs of (1, 2) *Talpa* cf. *T. minuta* from Studienka A de Blainville, 1840, (3) Urotrichini indet. from Triblavina, and (4–9) *Desmanodon* cf. *D. fluegeli* Prieto et al., 2010, from Borský Svätý Jur. (1) P4, ST214210; (2) M3, ST214212; (3) M1, TB170245; (4) P4, BJ213450; (5) M1, BJ213451; (6) M3, BJ213452; (7) m2, BJ213455; (8) m3, BJ213456; (9), m3, BJ213457. Images with underlined numbers are reversed.

**Diagnosis.**—See Prieto et al. (2010, p. 111).

**Occurrence.**—MN7/8 of Austria and MN9 of Slovakia (Prieto et al., 2010; this paper).

**Description.**—The P4 is a reduced tooth with a high paracone in an anterior position. The parastyle is a minute extension of the anterolabial border. At the center of the labial margin, a pointy cusplule is attached to the base of the paracone. This creates a small, open basin between this cusplule and the posterocrista. The latter is sharp and almost straight. It ends before reaching the posterior margin by displaying a thicker tip (metacone; Fig. 9.4). A low metastyle is present. The conical protocone is small and connected to the posterolingual cingulum. This cingulum stops beneath the posterolingual end of the posterocrista. Consequently, the P4 fits the morphotype A (sensu van den Hoek Ostende, 1989).

The M1 has a strong transversal development (Fig. 9.5). The parastyle is reduced and creates an angular anterolabial corner. The metacone is high and triangular in cross-section. This cusp leads posterolabially to a high and straight postmetacrista. An almost independent metastyle is attached to the anterior flank of the postmetacrista. On the posterolabial side of this crest, a second, independent, and pointy cusplule is present. The mesostyles are strongly separated. The lingual cusps are poorly differentiated. The protocone is high and anterolingually stretched. The protoconule is found near the protocone and is separated from it only by a superficial notch. The protoconule leads to two crests: the shorter posterior arm reaches the paracone whereas the slightly curved anterior arm ends at the anterior margin. The protocone is connected to a relatively low hypocone, from which starts a short posthypocrista ending at the middle of the oblique posterior border. On the posthypocrista, a hardly distinguishable bulge is found. The only available, subtriangular M3 is heavily worn (Fig. 9.6). The mesostyles are robust and clearly separated. The anterior branch of the paracone leads to a curved and eccentric parastyle. The hypocone is robust and well separated from the compressed metacone.

The anteroposteriorly compressed trigonid of the m2 is shorter and slightly narrower than the talonid (Fig. 9.7). The cusplids are high. The paralophid and the protolophid are similarly shaped. The talonid basin is extremely narrow. The entoconid is connected to the trigonid wall by a low ridge. The low oblique cristid reaches the middle part of the trigonid wall. The anterior cingulid is thick. The labial cingulid does not join the anterior one. The posterior cingulid only consists of a weak entostylid. The length of our two m3s equals 80.8% and 81.4% the length of m2. The trigonid has a configuration similar to the one of m2. As in m2, the m3 has high cusplids. The entoconid is only slightly higher than the hypoconid. The talonid basin is open and elliptical. The anterior cingulid is as strong as on m2 and not connected to the labial cingulid. There is no posterior cingulid.

**Material.**—Borský Svätý Jur: one P4 (L = 1.32, W = 1.05), one M1 (L = 1.70, W = 2.07), one M3 (L = 1.11, W = 1.55), one m2 (L = 1.72, W1 = 1.19, W2 = 1.07), two m3 (L = 1.39, W1 = 0.93, W2 = 0.87; L = 1.40, W1 = 0.88, W2 = 0.73).

**Remarks.**—The presence of a talpid with a reduced parastyle on P4 (Fig. 9.4) and a stretched M1 with strongly divided mesostyle (Fig. 9.5) is unexpected in the Late Miocene of Europe. These features are found in older deposits and correspond to the configuration of *Desmanodon* (see Engesser, 1980; van den Hoek Ostende, 1989; Prieto et al., 2010). Within *Desmanodon*, the species from Borský Svätý Jur is easily distinguishable from *D. major* and *D. larsi* by its smaller size, the more reduced parastyle on P4, and the incomplete posterior and anterior cingulum on M1; from *D. antiquus* and *D. burkarti* by its smaller size and weaker parastyle on M1; from *D. crocheti* by its smaller size and less strongly split mesostyles; from the similar-sized *D. zieglerei* by its weaker parastyle on M1, reduced lingual area, and incomplete posterior cingulum; and from the smaller *D. daamsi* by the more gracile cusp structure and more divided mesostyles. Stronger similarities are found with *D. minor* from the MN7/8 of Sarıçay but especially with *D. fluegeli* from the MN7/8 of Gratkorn. Namely the stretched protocone, reduced hypocone,

and incomplete anterior and posterior cingula on upper molars (Engesser, 1980; Prieto et al., 2010; Vasileiadou and Doukas, 2022). The material from Borský Svätý Jur can be distinguished from the type material of *D. fluegeli* by the lack of cingulum near the protocone on M1, the weaker labial cingulid on m2, and the overall smaller size: the mean length of our m2 and m3 both equal ~84% of the mean length of the type material. These morphological features are subject to variation, and it has been attested that the dimensions of the lower molars of *Desmanodon* can vary greatly (Engesser, 1980, fig. 63). In view of the minor differences, our material is attributed to *Desmanodon* cf. *D. fluegeli*.

## Discussion

The diversity of Talpidae from Slovakia confirms the high diversity in Eulipotyphla observed in Central Europe during the Late Miocene. Eleven species of Talpidae are identified in the Late Miocene of Slovakia (Table 7), which is equal to the number of identified species in Austria (Ziegler, 2006a). The last European occurrence of *Desmanodon* is attested in Borský Svätý Jur, demonstrating its survival into the Late Miocene. The northwestern margin of the Pannonian basins system may correspond to a refugium for the last European populations, the presence of which may represent a late migration of a *Desmanodon* species from Anatolia, given the similarity with the Turkish late Middle Miocene species *D. minor*. The Uropsilinae are continuously present throughout the Late Miocene of Slovakia; *Desmanella* being the most abundant talpid genus in numerous localities (number of identified specimens; Table 7). Additionally, the Desmanini are well represented in our samples with four species. The two species from Šalgovce 5 are not found elsewhere, which is most likely attributable to the scarcity of MN12-aged deposits in Central Europe.

The subfamily Talpinae represents an important part of the species richness of the family Talpidae in the early Late Miocene faunas from Slovakia and Austria. The material from Slovakia is distinct from the Austrian material by the lack of large forms, namely *Talpa vallesensis* and *Talpa* aff./cf. *T. gilothi*, alongside the urotrichine *Urotrichus giganteus* Ziegler, 2006a. *Urotrichus giganteus* is known only by humeri, which are poorly represented in our material, and *T. vallesensis* is only identified in the MN10 of Schernham. The maximal geographic distribution of the scalopine *Proscapanus* occurred in the

earliest Middle Miocene, where it is recorded from Spain (van den Hoek Ostende and Furió, 2005) to China (Tao, 2006; Qiu et al., 2013). The apparent retreat of this genus from Western Europe and Asia occurred during the late Middle Miocene. A stock of *Proscapanus* was, however, still present in the Carpathian area during the Late Miocene, as shown by *P. minor*, *P. austriacus*, and *P. metastylidus*. In the Vallesian of Slovakia, the remains of *Proscapanus* even represent 55% of all the Talpidae material (Table 7).

In Austria, Talpini are diverse and omnipresent in Late Miocene localities; Scalopini are more rarely recorded (Ziegler, 2006a). By opposition, in Slovakia, only few Talpini are found in a single locality (Studienka A) during the Vallesian, whereas Scalopini are relatively abundant in both Borský Svätý Jur and Studienka (number of identified specimens; Table 7). The Late Miocene localities with the highest specific diversity of Talpidae in Austria and Slovakia are the ones containing both tribes—namely, Richardshof-Golfplatz (RH-A/2), Studienka, Richardshof-Wald (Rh-94/1), and Schernham. This partly explains why the North Alpine Foreland and the Western Carpathians basins contain localities with high diversity compared to other European regions during the Late Miocene.

The common co-occurrence of Scalopini and Talpini in the region has several implications. Burrowing moles became a significant portion of talpid specific diversity during the Miocene. It is probable that the large spectrum of fossoriality inferred for mole tribes and genera (Schwermann and Thompson, 2015) led to a decrease in ecological niche overlap, therefore leading to an increase of the number of local species (Klietmann et al., 2015). However, Scalopini and Talpini have a very comparable dental morphology, and both tribes show an extreme adaptation to fully subterranean life, the latter being the result of convergent evolution (Schwermann and Thompson, 2015). Since Scalopini and Talpini are recorded in similar environments and display strongly similar ecomorphology (See Klietmann, 2013), they are likely occupying overlapping ecological niches.

A non-overlapping distribution of the Scalopini and Talpini would be coherent with the competitive exclusion principle, but this is not observed in the Late Miocene of Austria and, to a lesser degree, in Slovakia. Indeed, both tribes underwent contemporaneous diversifications. In the fauna of Schernham, where both tribes are similarly abundant (number of specimens and number of most-common elements; data according to Ziegler, 2006a),

**Table 7.** Composition of the Talpidae from the Late Miocene of Slovakia (in number of identified specimens).

	MN9		MN10	MN11		MN12	
	Borský Svätý Jur	Studienka		Triblavina	Krásno	Šalgovce	
		A	E			Pezinok	4
<b>Talpidae</b>							
<i>Desmanella rietscheli</i> Storch and Dahlmann, 2000	94	2 (cf.)	1 (cf.)				
<i>Desmanella dubia</i> Rümke, 1976					38 (cf.)	1 (cf.)	40
<i>Archaeodesmana vinea</i> (Storch, 1978)				2 (cf.)	12		
<i>Archaeodesmana dissona</i> n. sp.							34
<i>Gerhardstorchia biradicata</i> (Ziegler, 2006a)			6				
<i>Gerhardstorchia</i> sp.							2
<i>Proscapanus minor</i> Ziegler, 2006a	89	32					
<i>Proscapanus austriacus</i> Ziegler, 2006a		9					
<i>Talpa</i> cf. <i>T. minuta</i> de Blainville, 1840		2					
Urotrichini gen. and sp. indet.					2	1	
<i>Desmanodon</i> cf. <i>D. fluegeli</i> Prieto et al., 2010	6						

slight differences in size are observed among *Talpa* aff. *T. minuta* (mean Lm1 = 1.50), *Talpa vallesensis* (mean Lm1 = 1.79), *Proscapanus minor* (mean Lm1 = 1.88), and *Proscapanus austriacus* (mean Lm1 = 2.05). It is also worth noting that *P. austriacus* has a stouter dental morphology than *P. minor*. This supports the progressive acquisition of slightly different dietary preferences alongside a divergence in size (Fig. 8). The co-occurrence and diversification of these highly fossorial talpid species during the Vallesian suggests peculiarly favorable parameters, notably with regard to available resources.

Overall, the high morphological and specific diversities of talpid species support the presence of heterogeneous environments at the regional scale during the Vallesian. The strong decline of fossorial Talpidae in Austria and Slovakia during the latest Vallesian/early Turolian is followed by the growing success of Desmanini, a tribe with a lesser diversity that filled a completely different ecological niche (see Rümke, 1985). Only the generalist and probably litter-burrower (García-Alix et al., 2011) *Desmanella* remained unaffected during this period. The success of the water-moles in Šalgovce 5 (MN12) supports a change towards more homogeneous environments with a prevalence of lakes, low-energy rivers, and floodplains. Such interpretation matches the paleoenvironmental reconstruction of Joniak et al. (2020).

## Acknowledgments

We would like to thank M. Furió, an anonymous reviewer, editor J. Calede, and managing editor J. Kastigar for their helpful comments that significantly improved the manuscript. We are very grateful to U.B. Göhlich, W. Wessels, J. van Dam, and E. Robert for their help providing comparative material from the paleontological collections of Vienna, Utrecht, and Lyon. We are also grateful to T. Lehmann and J. Eberhardt for their great assistance when dealing with the tricky case of *Desmanella rietscheli*. We extend our thanks to M. Furió who provided bibliographic resources. This research was supported by grants UK/27/2022 and UK/221/2023 of Comenius University, the Scientific Grant Agency of the Ministry of Education, Science, Research and Sport of the Slovak Republic and Slovak Academy of Sciences (VEGA) under the contract VEGA 1/0533/21, the Slovak Research and Development Agency (projects APVV-20-0120 and APVV-20-0079), and the Austrian Science Funds (FWF) under the project P-15724-N06.

## Declaration of competing interest

The authors declare none.

## Data availability statement

Data available from the Dryad Digital Repository: <http://doi.org/10.5061/dryad.r2280gbk9>

## References

Bachmayer, F., and Wilson, R.W., 1978, A second contribution to the fossil small mammal fauna of Kohfidisch, Austria: *Annalen des Naturhistorischen Museums in Wien*, v. 81, p. 129–161.

- Bannikova, A., Zemlemerova, E.D., Colangelo, P., Sözen, M., Sevidik, M., Kidov, A.A., Dzuev, R.I., Kryštufek, B., and Lebedev, V.S., 2015, An underground burst of diversity—a new look at the phylogeny and taxonomy of the genus *Talpa* Linnaeus, 1758 (Mammalia: Talpidae) as revealed by nuclear and mitochondrial genes: *Zoological Journal of the Linnean Society*, v. 175, p. 930–948, <https://doi.org/10.1111/zoj.12298>.
- Bilgin, M., Joniak, P., Mayda, S., Göktaş, F., Kaya, T., Campomanes, P.P., and van den Hoek Ostende, L.W., 2019, Sabuncubeli too, Bornova, a second micromammal assemblage from the Sabuncubeli section (Early Miocene, western Anatolia): *Palaeobiodiversity and Palaeoenvironments*, v. 99, p. 655–671, <https://doi.org/10.1007/s12549-019-00395-2>.
- Cailleux, F., Joniak, P., and van den Hoek Ostende, L.W., 2023, The Late Miocene Erinaceidae (Eulipotyphla, Mammalia) from the Pannonian Region, Slovakia: *Journal of Paleontology*, v. 97, p. 777–798, <https://doi.org/10.1017/jpa.2023.50>.
- Crochet, J.-Y., 1986, Insectivores Pliocènes du sud de la France (Languedoc–Roussillon) et du nord-est de l’Espagne: *Palaeovertebrata*, v. 16, p. 145–171.
- Crochet, J.-Y., and Green, M., 1982, Contributions à l’étude des micromammifères du gisement Miocène Supérieur de Montredon (Hérault). Les insectivores: *Palaeovertebrata*, v. 12, p. 119–131.
- Dahlmann, T., 2001, Die Kleinsäuger der unter-pliozänen Fundstelle Wölferheim in der Wetterau (Mammalia: Lipotyphla, Chiroptera, Rodentia): *Courier Forschungsinstitut Senckenberg*, v. 227, p. 1–129.
- Dahlmann, T., and Doğan, S., 2011, *Gerhardstorchia* nomen novum: a new name for *Storchia* Dahlmann 2001 (Mammalia: Lipotyphla: Talpidae: Desmaninae): *Paläontologische Zeitschrift*, v. 85, p. 91–91, <https://doi.org/10.1007/s12542-010-0079-4>.
- de Blainville, H.M.D., 1840, Osteographie des mammifères insectivores (*Talpa*, *Sorex* et *Erinaceus* L.): *Osteographie des Mammifères*, v. 1, p. 1–115.
- Dobson, G.E., 1883, A Monograph of the Insectivora, Systematic and Anatomical: London, John van Voorst, v. 2, p. 86–172.
- Doukas, C.S., van den Hoek Ostende, L.W., Theodoropoulos, C.D., and Reumer, J.W.F., 1995, The vertebrate locality Maramena (Macedonia, Greece) at the Turolian–Ruscinian boundary (Neogene): *Münchener Geowissenschaftliche Abhandlungen*, v. 28, p. 43–64.
- Engesser, B., 1972, *Die obermiozäne säugetierfauna von Anwil (Baselland)* [Ph.D. thesis]: University of Basel, Liestal, Switzerland, Lüdén A.G., 363 p.
- Engesser, B., 1980, Insectivora und Chiroptera (Mammalia) aus dem Neogen der Türkei: *Schweizerische Paläontologische Abhandlungen*, v. 102, p. 47–159.
- Engesser, B., 2009, The insectivores (Mammalia) from Sansan (Middle Miocene, south-western France): *Schweizerische Paläontologische Abhandlungen*, v. 128, p. 1–91.
- Fejfar, O., and Sabol, M., 2005, Czech Republic and Slovak Republic, in van den Hoek Ostende, L.W., Doukas, C.S., and Reumer, J.W.F., eds., *The Fossil Record of the Eurasian Neogene Insectivores (Erinaceomorpha, Soricomorpha, Mammalia)*, Part I: *Scripta Geologica Special Issue*, v. 5, p. 51–60.
- Fischer, G., 1814, *Zoognosia Tabulis Synopticis Illustrata, Volumen Tertium: Quadrupedum Reliquorum, Cetorum et Monotrymatum Descriptionem Continens*: Moscow, Nicolai Sergeidis Vsevolozsky, 732 p.
- Freudenberg, W., 1914, Die Säugetiere des Altern Quartärs von Mitteleuropa mit besonderer Berücksichtigung der Faunen von Hundsheim und Deutsch-Altenburg in Niederösterreich nebst Bemerkungen über verwandte Formen anderer Fundorte: *Geologische und Paläontologische Abhandlungen*, v. 12, p. 455–670.
- Furió, M., 2007, *Los insectívoros (Soricomorpha, Erinaceomorpha, Mammalia) del Neógeno Superior del Levante Ibérico* [Ph.D. thesis]: Barcelona, Spain, Universitat Autònoma de Barcelona, 299 p.
- Furió, M., Van Dam, J., and Kaya, F., 2014, New insectivores (Lipotyphla, Mammalia) from the Late Miocene of the Sivas Basin, Central Anatolia: *Bulletin of Geosciences*, v. 89, p. 163–181, <https://doi.org/10.3140/bull.geosci.1472>.
- Gaillard, C., 1899, Mammifères Miocènes nouveaux ou peu connus de La Grive–Saint-Alban (Isère): *Archives du Muséum d’Histoire Naturelle de Lyon*, v. 7, 78 p.
- García-Alix, A., Furió, M., Minwer-Barakat, R., Martín Suarez, E., and Freudenthal, M., 2011, Environmental control on the biogeographical distribution of *Desmanella* (Soricomorpha, Mammalia) in the Miocene of the Iberian Peninsula: *Palaeontology*, v. 54, p. 753–762.
- Gibert, J., 1975, New insectivores from the Miocene of Spain: *Proceedings van de Koninklijke Nederlandse Akademie van Wetenschappen*, v. 78, p. 108–133.
- Harrison, D.L., and Rzebik-Kowalska, B., 1994, A note on the occurrence of *Desmanella* cf. *dubia* Rümke, 1976 (Insectivora: Talpidae: Uropsilinae) in the Lower Pliocene of Podlesice, Poland: *Cranium*, v. 11, p. 3–6.
- He, K., Shinohara, A., Helgen, K.M., Springer, M.S., Jiang, X.L., and Campbell, K.L., 2016, Talpid mole phylogeny unites shrew moles and illuminates overlooked cryptic species diversity: *Molecular Biology and Evolution*, v. 34, p. 78–87, <https://doi.org/10.1093/molbev/msw221>.

- Hutchison, J.H., 1974, Notes on type specimens of European Miocene Talpidae and a tentative classification of old world Tertiary Talpidae (Insectivora: Mammalia): *Geobios*, v. 7, p. 211–256.
- Joniak, P., 2005, *New rodent assemblages from the Upper Miocene deposits of the Vienna Basin and Danube Basin* [thesis]: Bratislava, Slovakia, Department of Geology and Paleontology, Faculty of Natural Sciences, Comenius University in Bratislava, p. 1–126.
- Joniak, P., 2016, Upper Miocene rodents from Pezinok in the Danube Basin, Slovakia: *Acta Geologica Slovaca*, v. 8, p. 1–14.
- Joniak, P., and Šujan, M., 2020, Systematic and morphometric data of Late Miocene rodent assemblage from Triblavina (Danube Basin, Slovakia): *Data in Brief*, v. 28, e104961. <https://doi.org/10.1016/j.dib.2019.104961>.
- Joniak, P., Šujan, M., Fordinál, K., Braucher, R., Rybár, S., Kováčová, M., Kováč, M., and Aster Team, 2020, The age and paleoenvironment of a Late Miocene floodplain alongside Lake Pannon: rodent and mollusk biostratigraphy coupled with authigenic  $^{10}\text{Be}/^9\text{Be}$  dating in the northern Danube Basin of Slovakia: *Palaeogeography, Palaeoclimatology, Palaeoecology*, v. 538, e109482. <https://doi.org/10.1016/j.palaeo.2019.109482>.
- Kälin, D., and Engesser, B., 2001, Die jungmiozäne Säugetierfauna vom Nebelbergweg bei Nunningen (Kanton Solothurn, Schweiz): *Schweizerische Paläontologische Abhandlungen*, v. 121, p. 1–6.
- Klietmann, J., 2013, *Systematic and ecological analysis of Marsupialia and Eulipotyphla from Petersbuch 28 (Germany, Lower Miocene)* [Ph.D. thesis]: Vienna, Austria, University of Vienna, 484 p.
- Klietmann, J., Metscher, B.D., van den Hoek Ostende, L.W., Nagel, D., and Rummel, M., 2013, First record of an upper deciduous molar in *Desmanella* (Uropilinae, Talpidae, Mammalia): *Geobios*, v. 46, p. 503–510. <https://doi.org/10.1016/j.geobios.2013.07.005>.
- Klietmann, J., Nagel, D., Rummel, M., and van den Hoek Ostende, L.W., 2015, A gap in digging: the Talpidae of Petersbuch 28 (Germany, Early Miocene): *Paläontologische Zeitschrift*, v. 89, p. 563–592. <https://doi.org/10.1007/s12542-014-0228-2>.
- Kormos, T., 1913, Trois nouvelles especes fossiles des Desmans en Hongrie: *Annales Historico-naturales Musei Nationalis Hungarici*, v. 11, p. 135–145.
- Kormos, T., 1930, Diagnosen neuer Säugetiere aus dem Oberpliocänen fauna des Somlyőberges bei Püspökfürdő: *Annales Musei Nationalis Hungarici*, v. 27, p. 237–246.
- Lartet, E., 1851, Notice sur la colline de Sansan: *Annuaire du Département du Gers*, 42 p.
- Linnaeus, C., 1758, *Systema Naturae per Regna Tria Naturae* (tenth edition), Volume 1, *Regnum Animale*: Stockholm, Laurentii Salvii, 824 p.
- Martín-Suárez, E., Bendala, N., and Freudenthal, M., 2001, *Archaeodesmana baetica*, sp. nov. (Mammalia, Insectivora, Talpidae) from the Mio–Pliocene transition of the Granada Basin, southern Spain: *Journal of Vertebrate Paleontology*, v. 21, p. 547–554.
- Mayr, H., and Fahlbusch, V., 1975, Eine unterpliocäne Kleinsäugerfauna aus der Oberen Süßwasser–Molasse Bayerns: *Mitteilungen der Bayerischen Staatssammlung für Paläontologie und Historische Geologie*, v. 15, p. 91–111.
- Mein, P., 1999, The Late Miocene small mammal succession from France, with emphasis on the Rhône Valley localities, in Agustí, J., Rook, L., and Andrews, P., eds., *Hominoid Evolution and Climatic Change in Europe*, 1: Cambridge University Press, p. 140–164.
- Ménouret, B., and Mein, P., 2008, Les vertébrés du Miocène supérieur de Soblay (Ain, France): *Travaux et Documents des Laboratoires de Géologie de Lyon*, v. 165, p. 3–97.
- Minwer-Barakat, R., García-Alix, A., and Freudenthal, M., 2008, Desmaninae (Talpidae, Mammalia) from the Pliocene of Tollo de Chiclana (Guadix Basin, Southern Spain): *Considerations on the phylogeny of the genus Archaeodesmana*. *Geobios*, v. 41, p. 381–398. <https://doi.org/10.1016/j.geobios.2007.08.001>.
- Minwer-Barakat, R., García-Alix, A., Martín-Suárez, E., and Freudenthal, M., 2020, Early Pliocene Desmaninae (Mammalia, Talpidae) from southern Spain and the origin of the genus *Desmana*: *Journal of Vertebrate Paleontology*, v. 40, n. e1835936. <https://doi.org/10.1080/02724634.2020.1835936>.
- Norris, R.W., and Kilpatrick, C.W., 2007, A high elevation record of the star-nosed mole (*Condylura cristata*) in northeastern Vermont: *The Canadian Field-Naturalist*, v. 121, p. 206–207.
- Oudemans, A.C., 1923, *Acarologische Aanteekeningen*. LXXX: *Entomologische Berichten* (Amsterdam), v. 6, p. 145–155.
- Petényi, S.J., 1864, *Hátrahagyott munkái*: Pest, MTA Kiadósa, 130 p.
- Piras, P., Sansalone, G., Teresi, L., Kotsakis, T., Colangelo, P., and Loy, A., 2012, Testing convergent and parallel adaptations in talpids humeral mechanical performance by means of geometric morphometrics and finite element analysis. *Journal of Morphology*, v. 273, p. 696–711. <https://doi.org/10.1002/jmor.20015>.
- Prieto, J., 2010, The Middle Miocene mole *Desmanodon crocheti* sp. nov. (Talpidae, Mammalia): the last representative of the genus in the North Alpine foreland basin: *Paläontologische Zeitschrift*, v. 84, p. 217–225. <https://doi.org/10.1007/s12542-009-0038-0>.
- Prieto, J., Gross, M., Böhmer, C., and Böhme, M., 2010, Insectivores and bat (Mammalia) from the late Middle Miocene of Gratkorn (Austria): biostratigraphic and ecologic implications: *Neues Jahrbuch für Geologie und Paläontologie*, v. 258, p. 107–119. <https://doi.org/10.1127/0077-7749/2010/0088>.
- Prieto, J., van den Hoek Ostende, L.W., Hír, J., and Kordos, L., 2015, The Middle Miocene insectivores from Hasznos (Hungary, Nógrád County): *Palaeobiodiversity and Palaeoenvironments*, v. 95, p. 431–451.
- Qiu, Z.D., 1996, *Middle Miocene Micromammalian Fauna from Tunggur, Inner Mongolia*: Beijing, Science Press, 216 p.
- Qiu, Z.D., Wang, X., and Li, Q., 2013, Neogene faunal succession and biochronology of central Nei Mongol (Inner Mongolia), in Wang, X., Flynn, L., and Fortelius, M., *Fossil Mammals of Asia*: New York, Columbia University Press, v. 1, p. 155–186.
- Radulescu, C., Samson, P., and Ştiuca, E., 1989, Pliocene (lower Romanian) micromammals in the Dacic Basin: *Miscellanea Speologica Romanica*, v. 1, p. 313–326.
- Rümke, C.G., 1974, A new *Desmanella* species (Talpidae, Insectivora) from the Turolian of Conclud and Los Mansuetos (Prov. of Teruel, Spain): *Proceedings of the Koninklijke Nederlandse Akademie van Wetenschappen*, B, v. 77, p. 359–374.
- Rümke, C.G., 1976, Insectivora from Pikermi and Biodrak (Greece): *Proceedings of the Koninklijke Nederlandse Akademie van Wetenschappen*, B, v. 79, p. 256–270.
- Rümke, C.G., 1985, A review of fossil and recent Desmaninae (Talpidae, Insectivora): *Utrecht Micropaleontological Bulletins, Special Publication*, v. 4, 264 p.
- Rzebik-Kowalska, B., 2005, Erinaceomorpha and Soricomorpha (Mammalia) from the Miocene of Belchatów, Poland. IV. Erinaceidae Fischer von Waldheim, 1817 and Talpidae Fischer von Waldheim, 1817: *Acta Zoologica Cracoviensia*, v. 48, p. 71–91.
- Rzebik-Kowalska, B., and Lungu, A., 2009, Insectivore mammals from the Late Miocene of the Republic of Moldova: *Acta Zoologica Cracoviensia—Series A: Vertebrata*, v. 52, p. 11–60. [https://doi.org/10.3409/azc.52a\\_1-2.11-60](https://doi.org/10.3409/azc.52a_1-2.11-60).
- Rzebik-Kowalska, B., and Pawłowski, J., 1994, *Ruemkella* (Mammalia, Insectivora, Talpidae) nom. nov. for *Dibolia* Rümke, 1985 (nec Latreille, 1829): *Acta Zoologica Cracoviensia*, v. 37, p. 75–76.
- Rzebik-Kowalska, B., and Rekovets, L.I., 2016, New data on Eulipotyphla (Insectivora, Mammalia) from the Late Miocene to the middle Pleistocene of Ukraine: *Palaeontologia Electronica*, v. 19. <https://doi.org/10.26879/573>.
- Sabol, M., 2005, Middle Miocene assemblage of insectivores from Bonanza site near Devínska Nová Ves (Slovakia): *Geologica Carpathica Bratislava*, v. 56, p. 433–445.
- Sabol, M., Joniak, P., Bilgin, M., Bonilla-Salomón, I., Cailleux, F., Čerňanský, A., Malčková, V., Šedivá, M., and Tóth, C., 2021, Updated Miocene mammal biochronology of Slovakia: *Geologica Carpathica*, v. 72, p. 425–443. <https://doi.org/10.31577/GeolCarp.72.5.5>.
- Sansalone, G., Colangelo, P., Kotsakis, T., Loy, A., Castiglia, R., Bannikova, A.A., Zemlemerova, E.D., and Piras, P., 2018, Influence of evolutionary allometry on rates of morphological evolution and disparity in strictly subterranean moles (Talpinae, Talpidae, Lipotyphla, Mammalia): *Journal of Mammalian Evolution*, v. 25, p. 1–14. <https://doi.org/10.1007/s10914-016-9370-9>.
- Schreuder, A., 1940, A revision of the fossil water moles (Desmaninae): *Archives Néerlandaises de Zoologie*, v. 7, p. 202–333.
- Schwermann, A.H., and Thompson, R.S., 2015, Extraordinarily preserved talpids (Mammalia, Lipotyphla) and the evolution of fossoriality: *Journal of Vertebrate Paleontology*, v. 35, n. e934828. <https://doi.org/10.1080/02724634.2014.934828>.
- Storch, G., 1978, Die turoliche Wirbeltierfauna von Dorn–Dürkheim, Rheinhessen (SW-Deutschland), 2, Mammalia: Insectivora: *Senckenbergiana Lethaea*, v. 58, p. 421–449.
- Storch, G., and Dahlmann, T., 2000, *Desmanella rietscheli*, ein neuer Talpide aus dem Obermiozän von Dorn Dürkheim 1, Rheinhessen (Mammalia, Lipotyphla): *Carolinea*, v. 58, p. 65–69.
- Šujan, M., Braucher, R., Kováč, M., Bourlès, D. L., Rybár, S., Guillo, V., and Hudáčková, N., 2016, Application of the authigenic  $^{10}\text{Be}/^9\text{Be}$  dating method to Late Miocene–Pliocene sequences in the northern Danube Basin (Pannonian Basin System): confirmation of heterochronous evolution of sedimentary environments: *Global and Planetary Change*, v. 137, p. 35–53. <https://doi.org/10.1016/j.gloplacha.2015.12.013>.
- Tao, D., 2006, Chinese Neogene mammal biochronology: *Vertebrata Palasiatica*, v. 44, p. 143–163.
- Terzea, E., 1980, Deux micromammifères du Pliocène de Roumanie: *Travaux de l'Institut de Spéologie "Émile Racovitză"*, v. 19, p. 191–201.
- Thomas, O., 1912, On a collection of small mammals from the Tsinling Mountains, Central China, presented by Mr. G. Fenwick Owen to the National Museum: *Annals and Magazine of Natural History*, v. 10, p. 395–403.

- Topachevski, V.A., 1961, Novyi Plotsenovykh vid vykhukholi iz predkavkazya [A new water-mole from the Pliocene]: Paleontological Journal, v. 4, p. 131–137.
- Topachevsky, V., and Pashkov, A., 1983, Superspecific systematics of the genus *Desmana* (Insectivora, Talpidae): Vestnik Zoologii, v. 3, p. 39–45.
- Trouessart, E.-L., 1879, Catalogue des Mammifères vivants et fossiles III. Insectivora: Revue et Magasin de Zoologie Pure et Appliquée, ser. 3, v. 7, p. 219–285.
- van den Hoek Ostende, L.W., 1989, The Talpidae (Insectivora, Mammalia) of Eggingen–Mittelhart (Baden–Württemberg, F.R.G.) with special reference to the *Paratalpa–Desmanodon* lineage: Stuttgarter Beiträge zur Naturkunde B, v. 152, p. 1–29.
- van den Hoek Ostende, L.W., 1997, Insectivore faunas from the Lower Miocene of Anatolia. Part 4: the genus *Desmanodon* (Talpidae) with the description of a new species from the Lower Miocene of Spain: Proceedings of the Koninklijke Nederlandse Akademie van Wetenschappen, v. 100, p. 27–65.
- van den Hoek Ostende, L.W., and Fejfar, O., 2006, Erinaceidae and Talpidae (Erinaceomorpha, Soricomorpha, Mammalia) from the Lower Miocene of Merkur–Nord (Czech Republic, MN 3): Beiträge zur Paläontologie, v. 30, p. 175–203.
- van den Hoek Ostende, L.W., and Furió, M., 2005, Spain, in van den Hoek Ostende, L.W., Doukas, C.S., and Reumer, J.W.F., eds, The Fossil Record of the Eurasian Neogene Insectivores (Erinaceomorpha, Soricomorpha, Mammalia), Part I: Scripta Geologica Special Issue 5, p. 149–284.
- Vasileiadou, K., and Doukas, C.S., 2022, The fossil record of insectivores (Mammalia: Eulipotyphla) in Greece, in Vlachos E., ed., Fossil Vertebrates of Greece, Vol. 2: Cham, Springer, p. 33–92.
- Villalta, J.F., and Crusafont, M., 1944, Nuevos insectívoros del Mioceno continental del Vallés-Panadés: Notas y Comunicaciones del Instituto Geológico y Minero de España, v. 12, p. 39–65.
- Waddell, P.J., Okada, N., and Hasegawa, M., 1999, Towards resolving the interordinal relationships of placental mammals: Systematic Biology, v. 48, p. 1–5.
- Ziegler, R., 1985, Talpiden (Mammalia, Insectivora) aus dem Orleanium und Astaracium Bayerns: Mitteilungen der Bayerischen Staatssammlung für Paläontologie und Historische Geologie, v. 25, p. 131–175.
- Ziegler, R., 1990, Talpidae (Insectivora, Mammalia) aus dem Oberoligozän und Untermiozän Süd-Deutschlands: Stuttgarter Beiträge Naturkunde B, v. 167, p. 1–81.
- Ziegler, R., 1994, Bisher übersehene Insectivora (Mammalia) aus dem Untermiozän von Wintershof–West bei Eichstätt (Bayern): Mitteilungen der Bayerischen Staatssammlung für Paläontologie und Historische Geologie, v. 34, p. 291–306.
- Ziegler, R., 1998, Marsupialia und Insectivora (Mammalia) aus den oberoligozänen Spaltenfüllungen Herrlingen 8 und Herrlingen 9 bei Ulm (Baden–Württemberg): Senckenbergiana Lethaea, v. 77, p. 101–143.
- Ziegler, R., 2003, Moles (Talpidae) from the late Middle Miocene of South Germany: Acta Palaeontologica Polonica, v. 48, p. 617–648.
- Ziegler, R., 2005, The insectivores (Erinaceomorpha and Soricomorpha, Mammalia) from the Late Miocene hominoid locality Rudabánya: Palaeontographia Italica, v. 90, p. 53–81.
- Ziegler, R., 2006a, Insectivores (Lipotyphla) and bats (Chiroptera) from the Late Miocene of Austria: Annalen des Naturhistorischen Museums in Wien, Serie A für Mineralogie und Petrographie, Geologie und Paläontologie, Anthropologie und Prähistorie, v. 1, p. 93–196.
- Ziegler, R., 2006b, Miocene insectivores from Austria and Germany—an overview: Beiträge zur Paläontologie, v. 30, p. 481–494.

Accepted: 30 November 2023